Towards geometric D6-brane model building on non-factorisable toroidal $\mathbb{Z}_4$-orbifolds

Mikel Berasaluce-González, Gabriele Honecker and Alexander Seifert

PRISMA Cluster of Excellence & Institut für Physik (WA THEP),
Johannes-Gutenberg-Universität, D-55099 Mainz, Germany

E-mail: mberasal@uni-mainz.de, Gabriele.Honecker@uni-mainz.de,
alseifer@uni-mainz.de

ABSTRACT: We present a geometric approach to D-brane model building on the non-factorisable torus backgrounds of $T^6/\mathbb{Z}_4$, which are $A_3 \times A_3$ and $A_3 \times A_1 \times B_2$. Based on the counting of 'short' supersymmetric three-cycles per complex structure *vev*, the number of physically inequivalent lattice orientations with respect to the anti-holomorphic involution $\mathcal{R}$ of the Type IIA/$\Omega\mathcal{R}$ orientifold can be reduced to three for the $A_3 \times A_3$ lattice and four for the $A_3 \times A_1 \times B_2$ lattice. While four independent three-cycles on $A_3 \times A_3$ cannot accommodate phenomenologically interesting global models with a chiral spectrum, the eight-dimensional space of three-cycles on $A_3 \times A_1 \times B_2$ is rich enough to provide for particle physics models, with several globally consistent two- and four-generation Pati-Salam models presented here.

We further show that for fractional *sLag* three-cycles, the compact geometry can be rewritten in a $(T^2)^3$ factorised form, paving the way for a generalisation of known CFT methods to determine the vector-like spectrum and to derive the low-energy effective action for open string states.

Contents

1 Introduction

Ever since the finding in 1985 that string theory constitutes a framework for unifying quantum field theory and gravity, which — when compactified on a Calabi-Yau-threefold or some singular limit thereof such as a toroidal orbifold — leads to $\mathcal{N} = 1$ supersymmetry in four dimensions [1], the search for vacuum configurations with not only the Standard Model spectrum but also its interactions has been intensively pursued. Starting from sporadic models of the $E_8 \times E_8$ heterotic string such as [2, 3], by implementing systematic computer searches, large classes of vacua with particle physics spectra on $T^6/\mathbb{Z}_N$ and $T^6/\mathbb{Z}_N \times \mathbb{Z}_M$ orbifolds [4–6] (see also [7] for the heterotic SO(32) string theory) and Calabi-Yau manifolds [8–12] could be constructed.

    With the identification of D-branes as dynamical objects in Type I and II string theory [13] in 1995, model building also opened up in these theories, which are conjectured

to be related by S-duality [14, 15] and M-/F-theory duality [16, 17] to the vacua of the heterotic string. The virtue of D-brane model building lies in the fact that physical quantities, like e.g. the number of particle generations, are expressed in terms of topology and geometry of the compact space, which is particularly intuitive for the case of D6-branes on three-cycles in Type IIA orientifold compactifications, see e.g. [18] for a broad recent overview. This intuition, however, comes at the cost of the relatively little explored symplectic structure of generic Calabi-Yau threefolds. Since supersymmetric — or mathematically expressed *special Lagrangian* (*sLag*) — three-cycles constitute a largely unexplored area (except for [19, 20] and [21]), intersecting D6-brane models in Type IIA orientifolds have focussed on tori and toroidal orbifolds, and more specifically on backgrounds which are factorised into two-tori, $T^6 = (T^2)^3$, see e.g. [22–24], and $(T^2)^3/\Gamma$ with Abelian point groups $\Gamma = \mathbb{Z}_N$ or $\mathbb{Z}_N \times \mathbb{Z}_M$. In the latter case, models with all three-cycles inherited from the underlying torus have been constructed for $\Gamma = \mathbb{Z}_2 \times \mathbb{Z}_2$ [25–30] and $\mathbb{Z}_2 \times \mathbb{Z}_4$ [31–33] without discrete torsion, while fractional three-cycles consisting of components inherited from the torus plus exceptional divisors at orbifold singularities have been employed for $\Gamma = \mathbb{Z}_4$ [34], $\mathbb{Z}_6$ [33, 35–37], $\mathbb{Z}_6'$ [37–42] and $\mathbb{Z}_{12-II}$ [43] with a single $\mathbb{Z}_2$ sector and $\Gamma = \mathbb{Z}_2 \times \mathbb{Z}_2$ [44, 45], $\mathbb{Z}_2 \times \mathbb{Z}_6'$ [45–47] and $\mathbb{Z}_2 \times \mathbb{Z}_6$ [45, 48–50] with discrete torsion with two $\mathbb{Z}_2$ subgroups.

All of the above mentioned types of string vacua contain a plethora of scalar fields with flat directions. While the above models with a $\mathbb{Z}_2 \times \mathbb{Z}_2$ subsymmetry allow for *rigid* fractional three-cycles which, in the open string spectrum, provide gauge groups without brane recombination/splitting moduli in the adjoint representation, it has recently been noticed that (most) twisted complex structure moduli associated to deformations of singularities are in fact stabilised by the existence of D-branes with U(1) symmetries [50–53]. To further stabilise the dilaton and untwisted complex structure moduli, one usually argues that closed string background NS-NS fluxes (see [54–56] for reviews) provide a non-trivial scalar potential, see also [57, 58] for attempts to incorporate NS-NS fluxes on the factorisable $T^6/\mathbb{Z}_4$ orbifold and [59] for the factorisable $T^6/\mathbb{Z}_6'$ orbifold. However, incorporating a non-trivial NS-NS flux H_3 will in general violate the factorisation into two-tori and instead lead to so-called non-factorisable torus backgrounds [60–62].

Orbifolds of non-factorisable tori have, to our best knowledge, scarcely been considered in the literature. Within Type IIA orientifolds, one of the first studies of non-factorisable $\mathbb{Z}_N$ orbifolds can be found in [63], where special configurations of D6-branes on top of the O6-planes lead to a *local* cancellation of the RR tadpoles within the compact space. In [64] a similar analysis for $\mathbb{Z}_N \times \mathbb{Z}_M$ orbifolds was performed. In [65, 66] orientifolds of $T^6/(\mathbb{Z}_2 \times \mathbb{Z}_2)$ with (non-)factorisable lattices were considered, including D6-branes which are not parallel to the O6-planes, and in [43], three-cycles on the $D_4 \times A_2$ and $D_4 \times A_1 \times A_1$ lattices with $\mathbb{Z}_{12-I}$ and $\mathbb{Z}_{12-II}$ orbifold symmetry, respectively, were studied. Finally, in [67] the Yukawa couplings for a torus generated by a D_6 lattice were computed. Here, we will for the first time perform a thorough study of all possible *sLag* three-cycles on the two different non-factorisable lattice backgrounds $A_3 \times A_3$ and $A_3 \times A_1 \times B_2$ of $T^6/\mathbb{Z}_4$, for which we briefly provided some preliminary results in [68].

Besides from being able to classify *sLag* cycles on toroidal orbifolds, these geometrically simple backgrounds are equipped with the non-negligible power of allowing for an

explicit string quantisation and thus Conformal Field Theory (CFT) techniques, which do not only reproduce the RR tadpole cancellation conditions and chiral spectrum, but are indispensable for distinguishing gauge group enhancements $U(N) \hookrightarrow SO(2N)$ or $USp(2N)$ for D-branes wrapped on orientifold invariant three-cycles and for deriving the low-energy effective action (for particle physics models based on powerful RCFT techniques see e.g. also [69–72]). So far, CFT results within the geometrically intuitive approach to Type II string model building with D-branes have been obtained only for gauge couplings at one-loop and n-point couplings at tree-level using *bulk* cycles on the factorisable six-torus $(T^2)^3$ [73–78]. For *fractional* cycles on $(T^2)^3/\mathbb{Z}_N$ and $\mathbb{Z}_N \times \mathbb{Z}_M$ orbifolds [37, 79–81], the one-loop corrections to gauge couplings and the Kähler potential at leading order could be derived, while the one-loop corrections to the open string Kähler potential are only known for *bulk* cycles on such orbifolds [82], see also [45, 46, 48, 83] for the distinction of $U(N) \hookrightarrow SO(2N)$ versus $USp(2N)$ gauge group enhancement using one-loop gauge threshold computations. The aim of the present work is not only to generalise the geometric methods of deriving the chiral spectrum from topological intersection numbers, but also to initiate the generalisation of CFT techniques to so-called non-factorisable lattice backgrounds.

The outline of this article is as follows: in section 2 we first study the geometry of $T^6/\mathbb{Z}_4$ on non-factorisable tori, then implement anti-holomorphic involutions on the lattices to study orientifolds of Type IIA string theory in section 3, after which we proceed to discuss first hints on physical equivalences among different choices, and finally we study supersymmetric D6-branes wrapped on (fractional) three-cycles. In section 4, we argue that any supersymmetric fractional three-cycle on $T^6/\mathbb{Z}_4$ can be written in a factorised form, which paves the way for implementing CFT methods in order to distinguish gauge group enhancements $U(N) \hookrightarrow SO(2N)$ versus $USp(2N)$ and to derive the vector-like matter spectrum. We then proceed to provide some explicit Pati-Salam models with two and four particle generations in section 5. Section 6 contains our conclusions and outlook, and appendix A contains some further explicit examples of globally consistent D6-brane configurations with chiral matter on the $A_3 \times A_1 \times B_2$ lattice.

2 Non-factorisable $T^6/\mathbb{Z}_4$ orbifold geometries

In this section, we discuss the three-cycle geometry on the two non-factorisable background lattices, $A_3 \times A_3$ and $A_3 \times A_1 \times B_2$, of $T^6/\mathbb{Z}_4$. The $\mathbb{Z}_4$-action is usually encoded in the shift vector $\vec{\zeta} = \frac{1}{4}(1, -2, 1)$ if the six-torus is parameterized by three complex coordinates, and more generally the $\mathbb{Z}_4$-action is generated by the Coxeter element Q which acts on the root lattice of the corresponding orbifold spanned by the simple roots $\{e_i\}_{i=1,\ldots,6}$. Furthermore, we denote the six toroidal one-cycles along the directions $\{e_i\}$ by π_i and toroidal two- and three-cycles by $\pi_{ij} := \pi_i \wedge \pi_j$ and $\pi_{ijk} := \pi_i \wedge \pi_j \wedge \pi_k$, respectively. The Hodge numbers of all three possible lattice backgrounds — one factorisable and two non-factorisable ones — are summarized in table 1 (cf. e.g. [84]). We are in particular interested in characterization of the three-homology $H_3(T^6/\mathbb{Z}_4, \mathbb{Z})$ of each background lattice. This homology class contains in general the $\mathbb{Z}_4$-invariant bulk π^{bulk} and exceptional three-cycles π^{exc} as well as

Hodge numbers of $T^6/\mathbb{Z}_4$ orbifolds						
Lattice	h_{11}^{bulk}	$h_{11}^{\mathbb{Z}_2}$	$h_{11}^{\mathbb{Z}_4}$	h_{21}^{bulk}	$h_{21}^{\mathbb{Z}_2}$	$h_{21}^{\mathbb{Z}_4}$
$B_2 \times (A_1)^2 \times B_2$	5	10	16	1	6	0
$A_3 \times A_3$	5	4	16	1	0	0
$A_3 \times A_1 \times B_2$	5	6	16	1	2	0

Table 1. Summary of the Hodge numbers per untwisted and twisted sector of the $T^6/\mathbb{Z}_4$ orbifolds on factorisable and non-factorisable tori.

fractional linear combinations thereof, the so-called fractional three-cycles π^{frac}. The bulk three-cycles are inherited from the underlying torus and can be computed by taking the $\mathbb{Z}_4$-orbits thereof:

$$\pi^{\text{bulk}} := \sum_{i=0}^{i=3} Q^i \pi^{\text{torus}}. \tag{2.1}$$

The exceptional three-cycles arise for the $T^6/\mathbb{Z}_4$ orbifolds only in the $\mathbb{Z}_2$-twisted sector. They stem from the resolution of the $\mathbb{Z}_2$-invariant two-tori and can be written as a product of an exceptional two-cycle $\mathbf{e}_{\alpha\beta}$ (with $\alpha\beta$ labelling the location of the cycle) and a $\mathbb{Z}_2$-invariant toroidal one-cycle (plus some $\mathbb{Z}_4$-image). Finally, fractional three-cycles are either one-half of a bulk cycle or linear combinations of one-half of some bulk and exceptional three-cycles with the combinatorics depending on the corresponding singularities traversed by the bulk cycles as well as sign factors associated to the choice of some discrete Wilson line, or geometrically speaking the orientation the corresponding exceptional three-cycle is wrapped.

Based on the discussion in this section, we will proceed to discuss (supersymmetric) Type IIA orientifolds with O6-planes and D6-branes and the associated anti-holomorphic involution on the background geometry in section 3.

2.1 $B_2 \times (A_1)^2 \times B_2$

Before investigating the three-cycle geometry of the non-factorisable lattices, we briefly review three-cycles on the factorisable background on the group lattice $B_2 \times (A_1)^2 \times B_2$ as first discussed in [34], see e.g. also the appendix of [45] for the Hodge numbers per twist sector displayed in table 1. Although the B_2-torus is a square-torus, we take the positive simple roots of the B_2-Lie algebra as basis of the torus lattice (see figure 1). The $\mathbb{Z}_4$-action is then generated by the Coxeter element Q:

$$Q := \begin{pmatrix} 1 & -1 \\ 2 & -1 \end{pmatrix} \oplus \begin{pmatrix} -1 & 0 \\ 0 & -1 \end{pmatrix} \oplus \begin{pmatrix} 1 & -1 \\ 2 & -1 \end{pmatrix}, \tag{2.2}$$
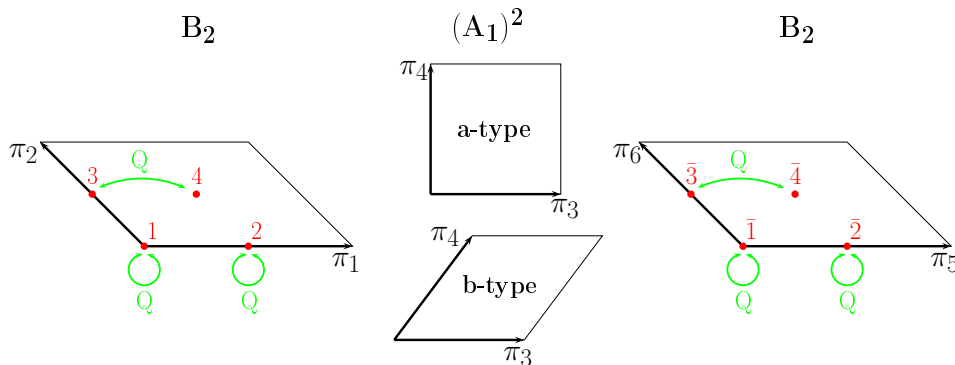
Figure 1. $T^6/\mathbb{Z}_4$-orbifold on the $B_2 \times (A_1)^2 \times B_2$-lattice and the $\mathbb{Z}_2$-invariant points (in red) on $T^2_{(1)} \times T^2_{(3)}$ with both possible shapes **a** and **b** displayed for the $(A_1)^2$ torus.

acting on three two-tori $T^2_{(i)}$. A basis of bulk three-cycles on the factorisable lattice is given by

$$
\gamma_1 := \sum_{k=0}^{3} Q^k (\pi_{235} + \pi_{236}) = 2\left(\pi_{136} + \pi_{235} + 2\pi_{236}\right),
$$

$$
\gamma_2 := -\sum_{k=0}^{3} Q^k \pi_{236} = 2\left(\pi_{135} + \pi_{136} + \pi_{235}\right),
$$

$$
\bar{\gamma}_1 := \sum_{k=0}^{3} Q^k (\pi_{245} + \pi_{246}) = 2\left(\pi_{146} + \pi_{245} + 2\pi_{246}\right),
$$

$$
\bar{\gamma}_2 := -\sum_{k=0}^{3} Q^k \pi_{246} = 2\left(\pi_{145} + \pi_{146} + \pi_{245}\right).
$$

(2.3)

An arbitrary bulk three-cycle can be represented by the (pairwise co-prime) toroidal wrapping numbers $(n^i, m^i)_{i=1,2,3}$,

$$
\begin{aligned}
\pi^{\text{bulk}} &= \sum_{k=0}^{3} Q^k \left(\bigwedge_{i=1}^{3} (n^i \pi_{2i-1} + m^i \pi_{2i}) \right) \\
&= An^2 \gamma_1 + Am^2 \bar{\gamma}_1 + Bn^2 \gamma_2 + Bm^2 \bar{\gamma}_2,
\end{aligned}
$$

(2.4)

where on the second line the $\mathbb{Z}_4$ invariant bulk wrapping numbers with

$$
A := n^1 m^3 + m^1 n^3 - 2n^1 n^3, \qquad B := n^1 m^3 + m^1 n^3 - m^1 m^3,
$$

(2.5)

have been used. The basic non-vanishing bulk intersection numbers are computed from

$$
\pi_a^{\text{bulk}} \circ \pi_b^{\text{bulk}} \equiv \frac{1}{4} \left(\sum_{i=0}^{3} Q^i \pi_a^{\text{torus}} \right) \circ \left(\sum_{i=0}^{3} Q^i \pi_b^{\text{torus}} \right) = \pi_a^{\text{torus}} \circ \left(\sum_{i=0}^{3} Q^i \pi_b^{\text{torus}} \right)
$$

(2.6)

and read

$$
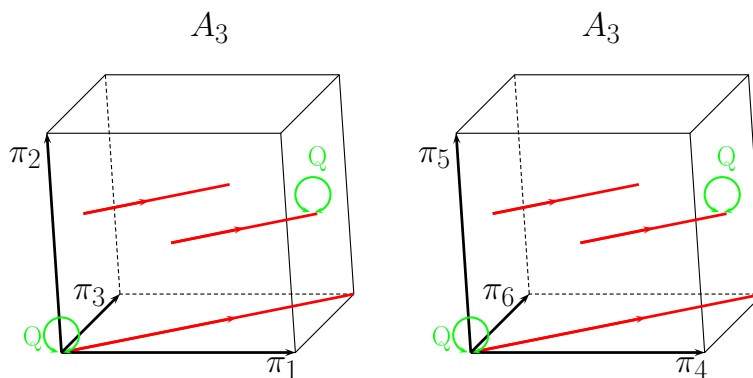\gamma_i \circ \bar{\gamma}_j = 2\, \delta_{ij}.
$$

(2.7)

Figure 2. $T^6/\mathbb{Z}_4$-orbifold on the $A_3 \times A_3$-lattice and its $\mathbb{Z}_2$-fixed lines (in red).

The bulk three-cycles thus do not form an unimodular basis. In addition to the bulk three-cycles, there exist twelve exceptional cycles with basis

$$\varepsilon_i = (e_{\alpha\beta} - e_{Q(\alpha)Q(\beta)}) \wedge \pi_3 \,, \qquad \bar{\varepsilon}_i = (e_{\alpha\beta} - e_{Q(\alpha)Q(\beta)}) \wedge \pi_4 \qquad (2.8)$$

(where α and β denote the $\mathbb{Z}_2$-invariant points on the four-torus $T^2_{(1)} \times T^2_{(3)}$ and $Q(\alpha)$ and $Q(\beta)$ their $\mathbb{Z}_4$ images), and with non-vanishing intersection numbers

$$\varepsilon_i \circ \bar{\varepsilon}_j = -2 \, \delta_{ij} \,. \qquad (2.9)$$

Fractional three-cycles of the form

$$\pi^{\text{frac}} = \frac{1}{2} \left(\pi^{\text{bulk}} + (-1)^{\tau^{\mathbb{Z}_2}} \sum_{\text{fixed set of } i} \left[\pm (n^2 \varepsilon_i + m^2 \bar{\varepsilon}_i) \right] \right), \qquad (2.10)$$

with the $\mathbb{Z}_2$ eigenvalue $(-1)^{\tau^{\mathbb{Z}_2}}$ parametrised by $\tau^{\mathbb{Z}_2} \in \{0, 1\}$ and the sum over four i such that the product of the signs $\pm$ gives $+1$, then generate the unimodular sixteen dimensional basis of three-cycles.

2.2 $A_3 \times A_3$

We start the discussion of non-factorisable $\mathbb{Z}_4$-orbifolds with the lattice of the type $A_3 \times A_3$ (see figure 2). The $\mathbb{Z}_4$ group acts by the Coxeter element Q on the vectors $\{e_i\}_{i=1,\dots,6}$, which span the six-torus:

$$\begin{aligned} Qe_1 &= e_2 \,, & Qe_2 &= e_3 \,, & Qe_3 &= -e_1 - e_2 - e_3 \,, \\ Qe_4 &= e_5 \,, & Qe_5 &= e_6 \,, & Qe_6 &= -e_4 - e_5 - e_6 \,, \end{aligned} \qquad (2.11)$$

which can be written in the matrix form

$$Q := \begin{pmatrix} 0 & 0 & -1 & 0 & 0 & 0 \\ 1 & 0 & -1 & 0 & 0 & 0 \\ 0 & 1 & -1 & 0 & 0 & 0 \\ 0 & 0 & 0 & 0 & 0 & -1 \\ 0 & 0 & 0 & 1 & 0 & -1 \\ 0 & 0 & 0 & 0 & 1 & -1 \end{pmatrix}. \qquad (2.12)$$

This action forms a discrete subgroup of SU(3) and thus preserves $\mathcal{N} = 2$ supersymmetry in four dimensions when compactifying Type II string theory. The Hodge numbers of this orbifold are (see e.g. [84]) $h_{21} = h_{21}^{\text{untw}} + h_{21}^{\mathbb{Z}_2} = 1 + 0$ and $h_{11} = h_{11}^{\text{untw}} + h_{11}^{\mathbb{Z}_4} + h_{11}^{\mathbb{Z}_2} = 5 + 16 + 4$ as displayed in the middle row in table 1. Due to $h_{21}^{\mathbb{Z}_2} = 0$, the three-homology of this orbifold contains only (fractions of) bulk three-cycles and is four-dimensional.

For the Q-action to be an isometry of the lattice, one has to require the invariance of the scalar product $Q^t g Q = g$ [85], which restricts the shape of the metric of the six-torus to

$$
g = \begin{pmatrix}
R_1^2 & aR_1^2 & -(2a+1)R_1^2 & eR_1R_2 & sR_1R_2 & cR_1R_2 \\
aR_1^2 & R_1^2 & aR_1^2 & dR_1R_2 & eR_1R_2 & sR_1R_2 \\
-(2a+1)R_1^2 & aR_1^2 & R_1^2 & cR_1R_2 & dR_1R_2 & eR_1R_2 \\
eR_1R_2 & dR_1R_2 & cR_1R_2 & R_2^2 & bR_2^2 & -(2b+1)R_2^2 \\
sR_1R_2 & eR_1R_2 & dR_1R_2 & bR_2^2 & R_2^2 & bR_2^2 \\
cR_1R_2 & sR_1R_2 & eR_1R_2 & -(2b+1)R_2^2 & bR_2^2 & R_2^2
\end{pmatrix} \tag{2.13}
$$

with $s := -(c + d + e)$. The moduli R_1 and R_2 describe the radii of $A_3 \times A_3$ whereas a (b) specifies the cosine of the angle between the vectors e_1 and e_2 $(e_4$ and $e_5)$ and c, d and e specify the cosines of the angles between e_4 and the vectors e_3, e_2 and e_1, respectively.

To describe the three-cycles on the six-torus T^6 we use the usual notation $\pi_{ikl} = \pi_i \wedge \pi_k \wedge \pi_l$. Due to the action of Q, it suffices to consider the three-cycles which wrap a two-cycle on one A_3-torus and a one-cycle on the other one. Such cycles can a priori be described by twelve wrapping numbers $(m^i, n^i, p^i, q^i, r^i, s^i)^{i=1,2}$:

$$
\pi^{\text{torus}} := (m^1\pi_1 + n^1\pi_2 + p^1\pi_3) \wedge (m^2\pi_1 + n^2\pi_2 + p^2\pi_3 + q^2\pi_4 + r^2\pi_5 + s^2\pi_6) \wedge (q^1\pi_4 + r^1\pi_5 + s^1\pi_6) . \tag{2.14}
$$

By taking orbits of the Q-action, the basis of $\mathbb{Z}_4$-invariant three-cycles is given by

$$
\begin{aligned}
\gamma_1 &:= \sum_{i=0}^{3} Q^i \pi_{124} = -\pi_{125} - \pi_{126} - \pi_{134} - \pi_{135} + \pi_{235} + \pi_{236} , \\
\gamma_2 &:= \sum_{i=0}^{3} Q^i \pi_{125} = \pi_{124} + \pi_{125} - \pi_{135} - \pi_{136} - \pi_{234} - \pi_{235} , \\
\bar{\gamma}_1 &:= \sum_{i=0}^{3} Q^i \pi_{145} = -\pi_{146} - \pi_{245} - \pi_{246} + \pi_{256} - \pi_{345} + \pi_{356} , \\
\bar{\gamma}_2 &:= \sum_{i=0}^{3} Q^i \pi_{245} = \pi_{145} - \pi_{156} + \pi_{245} - \pi_{246} - \pi_{256} - \pi_{346} .
\end{aligned} \tag{2.15}
$$

Using the ansatz (2.14) for a toroidal three-cycle, we can compute the corresponding bulk cycle with the orbifold map $\sum_{i=0}^{3} Q^i$ and decompose it in the basis (2.15):

$$
\begin{aligned}
\pi^{\text{bulk}} = {} & \left(A_1(q^1 - s^1) - A_2(q^1 + r^1 - s^1) + A_3 r^1\right)\gamma_1 \\
& + \left(A_1 r^1 + A_2(q^1 - r^1 - s^1) - A_3(q^1 - s^1)\right)\gamma_2 \\
& + \left(B_1(m^1 - p^1) - B_2(m^1 + n^1 - p^1) + B_3 n^1\right)\bar{\gamma}_1 \\
& + \left(B_1 n^1 + B_2(m^1 - n^1 - p^1) - B_3(m^1 - p^1)\right)\bar{\gamma}_2
\end{aligned} \tag{2.16}
$$

with

$$A_1 := m^1 n^2 - n^1 m^2, \qquad A_2 := m^1 p^2 - p^1 m^2, \qquad A_3 := n^1 p^2 - p^1 n^2,$$
$$B_1 := q^2 r^1 - r^2 q^1, \qquad B_2 := q^2 s^1 - s^2 q^1, \qquad B_3 := r^2 s^1 - s^2 r^1.$$

It is easy to verify that the non-vanishing intersection numbers between the basis elements (2.15) are given by

$$\gamma_i \circ \bar{\gamma}_j = -\delta_{ij}, \tag{2.17}$$

where we used analogously to the factorised lattice background in section 2.1 that we can define the intersection number between two toroidal three-cycles π_a^{torus} and π_b^{torus} on T^6 as $\pi_a^{\text{torus}} \circ \pi_b^{\text{torus}} = \pi_a^{\text{torus}} \wedge \pi_b^{\text{torus}}/\text{Vol}(T^6)$ to arrive at the intersection number between two $\mathbb{Z}_4$-invariant bulk three-cycles

$$\pi_a \circ \pi_b = \frac{1}{4}\left(\sum_{i=0}^{3} Q^i \pi_a^{\text{torus}}\right) \circ \left(\sum_{i=0}^{3} Q^i \pi_b^{\text{torus}}\right). \tag{2.18}$$

Therefore, $\{\gamma_1, \gamma_2, \bar{\gamma}_1, \bar{\gamma}_2\}$ already builds the unimodular basis.

Despite this and the fact that this orbifold does not have any exceptional three-cycles, in order to compare with the other non-factorisable lattice in section 2.3 below, we can consider the special class of three-cycles, for which the toroidal building blocks are $\mathbb{Z}_2$-invariant, i.e. fractional three-cycles[1]

$$\pi^{\text{frac}} = \frac{1}{2}\pi^{\text{bulk}}. \tag{2.19}$$

Using the Q-transformation of the wrapping numbers

$$\begin{pmatrix} m^i, & n^i, & p^i \\ q^i, & r^i, & s^i \end{pmatrix}^{i=1,2} \quad \xrightarrow{Q} \quad \begin{pmatrix} -p^i, & m^i - p^i, & n^i - p^i \\ -s^i, & q^i - s^i, & r^i - s^i \end{pmatrix}^{i=1,2}, \tag{2.20}$$

we obtain the following condition. Any toroidal three-cycle π^{torus} of the form (2.14) is $\mathbb{Z}_2$-invariant if and only if

$$\begin{aligned}
r^1(A_1 + A_3) &= 0, & n^1(B_1 + B_3) &= 0, \\
(s^1 - r^1)A_3 &= q^1 A_1, & (p^1 - n^1)B_3 &= m^1 B_1, \\
(A_1 + A_3)(s^1 - q^1) &= 0, & (B_1 + B_3)(m^1 - p^1) &= 0, \\
(A_1 + A_3)s^1 &= (q^1 - r^1 + s^1)A_2, & (B_1 + B_3)p^1 &= (m^1 - n^1 + p^1)B_2.
\end{aligned} \tag{2.21}$$

Among this special class of three-cycles from $\mathbb{Z}_2$-invariant toroidal cycles, there are also those that satisfy $Q\pi^{\text{torus}} = -\pi^{\text{torus}}$. They do not contribute to the bulk cycles, or in

---

[1]This construction will be used in the next sections. We will see that if both A_3-tori are orthogonal to each other, any fractional three-cycle is Lagrangian.

Note also that for $T^6/(\mathbb{Z}_2 \times \mathbb{Z}_2)$ without discrete torsion, the unimodular basis is constructed analogously using $\mathbb{Z}_2 \times \mathbb{Z}_2$-invariant three-cycles $\pi^{\text{torus}} = \frac{1}{4}\pi^{\text{bulk}}$, cf. e.g. [86]. However, since Q as defined in (2.12) permutes toroidal one-cycles on $T^6/\mathbb{Z}_4$ non-trivially, here we have to restrict to a special subclass of all *a priori* allowed bulk three-cycles.

other words are trivial in the $H_3(T^6/\mathbb{Z}_4, \mathbb{Z})$ homology. Taking into account this fact, we can reduce the conditions (2.21) to

$$A_1 + A_3 = 0, \qquad\qquad B_1 + B_3 = 0,$$
$$(q^1 - r^1 + s^1)A_i = 0, \qquad (m^1 - n^1 + p^1)B_i = 0 \text{ for all } i. \tag{2.22}$$

Note that due to the above $\mathbb{Z}_2$-invariance constraints on the wrapping numbers, the basis of these fractional three-cycles coincides with the basis $\{\gamma_1, \gamma_2, \bar{\gamma}_1, \bar{\gamma}_2\}$.

Let us for example consider the toroidal three-cycle $\pi = (\pi_1 + \pi_2) \wedge (\pi_1 + \pi_3) \wedge (\pi_4 - \pi_6)$. Obviously, it is $\mathbb{Z}_2$-invariant and gives rise to the fractional three-cycle $\pi^{\text{frac}} = \pi + Q\pi = -2\gamma_1$ on $T^6/\mathbb{Z}_4$. Although the original cycle has coprime wrapping numbers and no other toroidal three-cycle π' exists such that $\pi = 2\pi'$, the corresponding bulk cycle $-2\gamma_1$ is non-coprime. This will play a role for computing the gauge group in the section 3.4.

2.3 $A_3 \times A_1 \times B_2$

Now we consider three-cycles on $T^6/\mathbb{Z}_4$ with the lattice of type $A_3 \times A_1 \times B_2$. The $\mathbb{Z}_4$-action is generated by the Coxeter element which acts on the root lattice spanned by the simple roots $\{e_i\}_{i=1,\dots,6}$ in the following way

$$Qe_1 = e_2, \qquad Qe_2 = e_3, \qquad Qe_3 = -e_1 - e_2 - e_3,$$
$$Qe_4 = -e_4, \qquad Qe_5 = e_5 + 2e_6, \qquad Qe_6 = -e_5 - e_6, \tag{2.23}$$

which can be cast in the matrix form

$$Q := \begin{pmatrix} 0 & 0 & -1 & 0 & 0 & 0 \\ 1 & 0 & -1 & 0 & 0 & 0 \\ 0 & 1 & -1 & 0 & 0 & 0 \\ 0 & 0 & 0 & -1 & 0 & 0 \\ 0 & 0 & 0 & 0 & 1 & -1 \\ 0 & 0 & 0 & 0 & 2 & -1 \end{pmatrix}. \tag{2.24}$$

Again, this action corresponds to a discrete subgroup of SU(3), and thus preserves $\mathcal{N} = 2$ supersymmetry in four dimensions when considering Type II string theory compactifications. The Hodge numbers of this orbifold are [84] $h_{21} = h_{21}^{\text{untw}} + h_{21}^{\mathbb{Z}_2} = 1 + 2$ and $h_{11} = h_{11}^{\text{untw}} + h_{11}^{\mathbb{Z}_4} + h_{11}^{\mathbb{Z}_2} = 5 + 16 + 6$ (see table 1). Thus, we expect four bulk and four exceptional three-cycles on this orbifold.

From solving the equation $Q^t g Q = g$ we obtain

$$g := e_i \cdot e_j = \begin{pmatrix} R_3^2 & aR_3^2 & -(1+2a)R_3^2 & dR_3R_1 & bR_3R_2 & cR_3R_2 \\ aR_3^2 & R_3^2 & aR_3^2 & -dR_3R_1 & -(b+2c)R_3R_2 & (b+c)R_3R_2 \\ -(1+2a)R_3^2 & aR_3^2 & R_3^2 & dR_3R_1 & -bR_3R_2 & -cR_3R_2 \\ dR_3R_1 & -dR_3R_1 & dR_3R_1 & R_1^2 & 0 & 0 \\ bR_3R_2 & -(b+2c)R_3R_2 & -bR_3R_2 & 0 & 2R_2^2 & -R_2^2 \\ cR_3R_2 & (b+c)R_3R_2 & -cR_3R_2 & 0 & -R_2^2 & R_2^2 \end{pmatrix}. \tag{2.25}$$

The real positive moduli R_3, R_1 and R_2 describe the radii of $A_3 \times A_1 \times B_2$, respectively, and a, b, c and d specify the cosines of angles between the vectors of the lattice. More precisely, a is the cosine of the angle between the vectors e_1 and e_2, d the cosine of the angle between e_1 and e_4, b (c) is the cosine of the angle between e_1 and e_5 (e_6).

Bulk three-cycles. We make the ansatz that any toroidal three-cycle is factorisable in the sense that it can be characterised *a priori* by ten wrapping numbers $(m^1, n^1, p^1, q^1) \times (m^2, n^2, p^2, q^2) \times (m^3, n^3)$ and written as

$$\pi^{\text{torus}} := \bigwedge_{i=1}^{2} (m^i \pi_1 + n^i \pi_2 + p^i \pi_3 + q^i \pi_4) \wedge (m^3 \pi_5 + n^3 \pi_6) . \qquad (2.26)$$

The last doublet (m^3, n^3) gives us the one-cycle on the B_2-torus. The two quadruplets (m^i, n^i, p^i, q^i) parametrise the two-cycle on $A_3 \times A_1$. It is easy to see that the representation of three-cycles by this ansatz is not unique, i.e. the same three-cycle can be described by different wrapping numbers, e.g. when permuting the indices $i = 1$ and 2.

By taking orbits of the Q-action, we can define a basis of the $\mathbb{Z}_4$-invariant *bulk* three-cycles

$$
\begin{aligned}
\gamma_1 &:= -\sum_{i=0}^{3} Q^i \pi_{136} = 2(\pi_{125} + \pi_{126} - \pi_{136} - \pi_{235} - \pi_{236}) , \\
\gamma_2 &:= -\sum_{i=0}^{3} Q^i \pi_{125} = 2(\pi_{126} + \pi_{135} + \pi_{136} - \pi_{236}) , \\
\bar{\gamma}_1 &:= \sum_{i=0}^{3} Q^i \pi_{146} = \pi_{145} + 2\pi_{146} + 2\pi_{245} + 2\pi_{246} + \pi_{345} , \\
\bar{\gamma}_2 &:= \sum_{i=0}^{3} Q^i \pi_{246} = -\pi_{145} + 2\pi_{246} + \pi_{345} + 2\pi_{346} .
\end{aligned}
\qquad (2.27)
$$

Note that here the linear combinations $\frac{1}{2}(\gamma_1 \pm \gamma_2)$ are also bulk cycles. The decomposition in the basis $\{\gamma_{1,2}, \bar{\gamma}_{1,2}\}$ of any bulk three-cycle inherited from a toroidal one of the type (2.26) is given by

$$
\begin{aligned}
\pi^{\text{bulk}} &= P\gamma_1 + Q\gamma_2 + \bar{P}\bar{\gamma}_1 + \bar{Q}\bar{\gamma}_2 \\
&= \left[(A_2 - A_3)m^3 + \frac{1}{2}(A_1 - 2A_2 + A_3)n^3 \right] \gamma_1 + \left[(A_2 - A_1)m^3 + \frac{1}{2}(A_1 - A_3)n^3 \right] \gamma_2 \\
&\quad + \left[(-B_1 + B_2 + B_3)m^3 + (B_1 - B_3)n^3 \right] \bar{\gamma}_1 + \left[(-B_1 - B_2 + B_3)m^3 + B_2 n^3 \right] \bar{\gamma}_2 ,
\end{aligned}
\qquad (2.28)
$$

with

$$
\begin{array}{ll}
A_1 := m^1 n^2 - n^1 m^2, & B_1 := m^1 q^2 - q^1 m^2, \\
A_2 := m^1 p^2 - p^1 m^2, & B_2 := n^1 q^2 - q^1 n^2, \\
A_3 := n^1 p^2 - p^1 n^2, & B_3 := p^1 q^2 - q^1 p^2.
\end{array}
\qquad (2.29)
$$

Using the formula for bulk intersection numbers (2.18), we obtain for the bulk basis of (2.27)

$$\gamma_i \circ \bar{\gamma}_j = -2\delta_{ij} , \qquad \gamma_i \circ \gamma_j = \bar{\gamma}_i \circ \bar{\gamma}_j = 0 , \qquad (2.30)$$

which shows that the integral basis of bulk three-cycles is not unimodular.
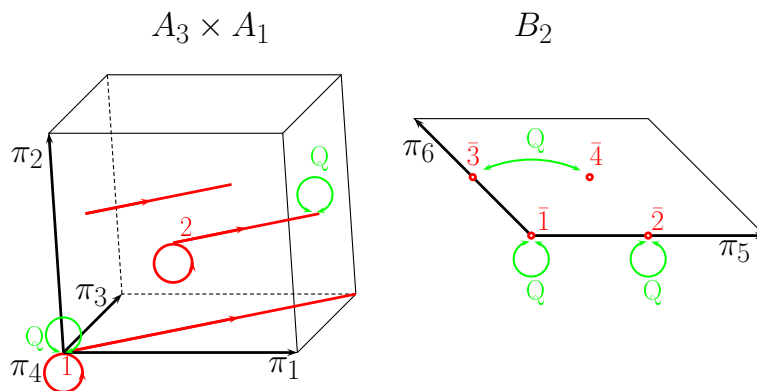
Figure 3. $T^6/\mathbb{Z}_4$-orbifold on the $A_3 \times A_1 \times B_2$-lattice and its $\mathbb{Z}_2$-fixed lines (in red).

Exceptional three-cycles. Besides the four bulk three-cycles $\gamma_i, \bar{\gamma}_i$ (with $i = 1, 2$), there are also four exceptional three-cycles appearing in the $\mathbb{Z}_2$ twisted sector of the orbifold. It is easy to see that Q^2 acts trivially on the sub-manifold $(\pi_1 + \pi_3) \wedge \pi_4$. One can show that there are eight such Q^2-invariant sub-manifolds, which are indicated in red in figure 3. We numerate them by $i\bar{j}$ where the first index denotes the $\mathbb{Z}_2$-invariant two-tori $(1, 2)$ on the $A_3 \times A_1$-torus and the second one the $\mathbb{Z}_2$-invariant points $(\bar{1}, \bar{2}, \bar{3}, \bar{4})$ on the B_2-torus. These Q^2-invariant sub-manifolds can be arranged in six congruence classes (under the Q-action): $\{1\bar{1}\}, \{1\bar{2}\}, \{1\bar{3}, 1\bar{4}\}, \{2\bar{1}\}, \{2\bar{2}\}, \{2\bar{3}, 2\bar{4}\}$.

The resolution of these six $\mathbb{Z}_2$-singular sub-manifolds gives rise to six four-dimensional sub-manifolds with the topology $S^2 \times T^2$ in accordance with $h_{22}^{\mathbb{Z}_2} \overset{\text{Poincaré}}{=} h_{11}^{\mathbb{Z}_2} = 6$ in table 1, where the exceptional two-cycle $\mathbf{e}_{i\bar{j}}$ describes the S^2-part, and the two one-cycles $\pi_1 + \pi_3$ and π_4 span a two-torus. The index of $\mathbf{e}_{i\bar{j}}$ is inherited from the numeration of the $\mathbb{Z}_2$-invariant two-tori. Finally by splitting T^2 into one-cycles $\pi_1 + \pi_3$ and π_4, we construct Q-invariant exceptional three-cycles. Due to the anti-symmetric action of Q on the one-cycles, only the exceptional two-cycles $\mathbf{e}_{1\bar{3}}, \mathbf{e}_{1\bar{4}}, \mathbf{e}_{2\bar{3}}, \mathbf{e}_{2\bar{4}}$ provide non-trivial results in the construction. Thus, the exceptional three-cycles are:

$$\gamma_3 := (\mathbf{e}_{1\bar{3}} - \mathbf{e}_{1\bar{4}}) \wedge (\pi_1 + \pi_3), \qquad \bar{\gamma}_3 := (\mathbf{e}_{1\bar{3}} - \mathbf{e}_{1\bar{4}}) \wedge \pi_4,$$
$$\gamma_4 := (\mathbf{e}_{2\bar{3}} - \mathbf{e}_{2\bar{4}}) \wedge (\pi_1 + \pi_3), \qquad \bar{\gamma}_4 := (\mathbf{e}_{2\bar{3}} - \mathbf{e}_{2\bar{4}}) \wedge \pi_4,$$

$$\tag{2.31}$$

with the intersection numbers

$$\gamma_i \circ \bar{\gamma}_j = 2\delta_{ij}, \qquad \gamma_i \circ \gamma_j = \bar{\gamma}_i \circ \bar{\gamma}_j = 0 \qquad i = 3, 4. \tag{2.32}$$

Since the intersection form of the γ_i's, and $\bar{\gamma}_i$'s ($i = 1, 2, 3, 4$) is not unimodular, these three-cycles do not form the minimal integral basis. We thus have to consider fractional three-cycles, which can consist of half a bulk cycle and simultaneously of half an exceptional cycle.

Fractional three-cycles and their integral basis. In order to write down an integral basis for the three-cycles such that the intersection form is unimodular, we start by specifying the construction of fractional cycles, which are $\mathbb{Z}_2$-invariant, analogously to the

factorisable case reviewed in section 2.1. The fractional cycles can wrap half a bulk cycle and half an exceptional one

$$\pi^{\text{frac}} = \frac{1}{2}\pi^{\text{bulk}} + \frac{1}{2}\pi^{\text{exc}}.$$

Motivated by the factorisable orbifold, we apply the well-known techniques of construction of the fractional cycles to our case. The non-factorisable structure of the lattice gives rise to some differences and therefore some modification of these techniques is needed.

In the case of the factorisable torus $T_1^2 \times T_2^2 \times T_3^2$, every $\mathbb{Z}_2$-invariant three-cycle passes through two $\mathbb{Z}_2$-invariant points per T^2 (here $T_1^2 \times T_3^2$) and contains a $\mathbb{Z}_2$-invariant one-cycle on the remaining two-torus (here T_2^2). In the $A_3 \times A_3$-case we saw that this does not hold true and we had to generalise this condition to $Q^2\pi^{\text{torus}} = \pi^{\text{torus}}$. The same happens in the present case of the $A_3 \times A_1 \times B_2$-lattice. Let us for example consider the toroidal cycle $(1,0,0,0) \times (0,0,0,1) \times (1,0) \equiv \pi_{145}$ through the origin. Despite the fact that this three-cycle contains the $\mathbb{Z}_2$-invariant one-cycle π_4 and passes through a $\mathbb{Z}_2$-invariant point, π_{145} is not $\mathbb{Z}_2$-invariant and therefore cannot be fractional. Indeed, one can check that $Q^2\pi_{145} = -\pi_{345}$. To impose the additional constraint on the numbers $(m^i, n^i, p^i, q^i)_{i=1,2} \times (m^3, n^3)$ ensuring the Q^2-invariance of the toroidal three-cycle we use the Q-action on the wrapping numbers

$$\begin{pmatrix} m^i, & n^i, & p^i, & q^i \\ & m^3, & n^3 & \end{pmatrix} \xrightarrow{Q} \begin{pmatrix} -p^i, & m^i - p^i, & n^i - p^i, & -q^i \\ & m^3 - n^3, & 2m^3 - n^3 & \end{pmatrix}. \tag{2.33}$$

For any toroidal three-cycle π^{torus} of the form (2.26), it can be shown that the following statements are equivalent:

$$\pi^{\text{torus}} \text{ is } \mathbb{Z}_2\text{-invariant} \iff Q^2\pi^{\text{torus}} = \pi^{\text{torus}} \iff A_1 + A_3 = 0 \text{ and } B_1 - B_2 + B_3 = 0. \tag{2.34}$$

Only such $\mathbb{Z}_2$-invariant toroidal three-cycles can be used for the construction of the fractional cycles. From the factorisable case we know that the toroidal three-cycles giving rise to the fractional cycles have to contain $\mathbb{Z}_2$-invariant one-cycles. Indeed, it can be verified that any cycle which satisfies the conditions (2.34) can be written as

$$(m^1, n^1, p^1, q^1) \times (m^2, n^2, p^2, q^2) \times (m^3, n^3) = (m^1, n^1, p^1, 0) \times (\tilde{p}^2, 0, \tilde{p}^2, \tilde{q}^2) \times (m^3, n^3) + \text{R}, \tag{2.35}$$

where $\tilde{p}^2 := p^2 - \frac{n^2}{n^1}p^1$ and $\tilde{q}^2 := q^2 - \frac{n^2}{n^1}q^1$ for $n^1 \neq 0$.[2] The remaining term

$$\text{R} := (0,0,0,q^1) \times (\tilde{p}^2, 0, \tilde{p}^2, \tilde{q}^2) \times (m^3, n^3)$$

does not contribute to the bulk three-cycle and can be neglected. Therefore, any $\mathbb{Z}_2$-invariant three-cycle contains a linear combination of the $\mathbb{Z}_2$-invariant one-cycles $\pi_1 + \pi_3$ and π_4.

The next step to construct the fractional cycles is to determine the exceptional part. In the factorisable case we identify which $\mathbb{Z}_2$-invariant points the toroidal three-cycle passes through. On the $A_3 \times A_1 \times B_2$-orbifold also the $\mathbb{Z}_2$-invariant lines are involved and so

---

[2] $n^1 = 0$ gives rise to a similar result.

we have to calculate their intersection with the toroidal three-cycle. Another important difference is that for the factorisable lattice $(T^2)^3$, the co-prime condition on the wrapping numbers (n^i, m^i) per T_i^2 is necessary and sufficient for the fractional cycle to have a co-prime decomposition in the unimodular basis. On the contrary, in the non-factorisable case the sufficiency condition gets lost and some further restrictions on the wrapping numbers (m^i, n^i, p^i, q^i) are needed. It turns out that it is convenient to neglect these constraints at first and better to select the co-prime cycles after they are expressed in the unimodular basis. Thus, in this case, for the computation of the exceptional part we have to know not just which $\mathbb{Z}_2$-invariant lines the toroidal three-cycle intersects but also how many times. That requires some combinatorics.

Using the property (2.35) for the $\mathbb{Z}_2$-invariant three-cycles, we have only to compute how many times the cycle with the wrapping numbers $(m^1, n^1, p^1, 0)$ intersects the one-cycle $\pi_1 + \pi_3$. We find that the number N of intersection points is

$$N = \text{g.c.d.}(m^1 - p^1, n^1). \tag{2.36}$$

Furthermore, we make the following considerations and set several notations:

- The three-cycle can pass through both fixed lines 1 and 2 on the A_3-torus if and only if $\frac{m^1-p^1}{N}$ and $\frac{n^1}{N}$ are odd. We introduce three new parameters counting the different fixed lines traversed by the three-cycle

$$\tau := \begin{cases} 2 & \text{if } \frac{m^1-p^1}{N} \text{ and } \frac{n^1}{N} \text{ are odd}, \\ 1 & \text{otherwise} \end{cases} \tag{2.37}$$

  and

$$\tau^1, \tau^2 \in \{0, 1\} \quad \text{with} \quad \tau^1 + \tau^2 = \tau. \tag{2.38}$$

- On the B_2-torus, a one-cycle with even wrapping number n^3 passes through the fixed points $\bar{1}$ and $\bar{2}$ (both $\mathbb{Z}_4$-invariant), or $\bar{3}$ and $\bar{4}$ (both $\mathbb{Z}_2$-invariant). In this case, the fractional three-cycle contains either none or two exceptional three-cycles. If n^3 is odd, the one-cycle on B_2 intersects one $\mathbb{Z}_4$- and one $\mathbb{Z}_2$-invariant fixed point, which in any case gives rise to one corresponding exceptional cycle. Thus, we define the parameter σ, which counts the number of exceptional three-cycles contributing to a fractional cycle for given bulk part, by

$$\sigma := \begin{cases} 0, 2 & \text{if } n^3 \text{ is even}, \\ 1 & \text{if } n^3 \text{ is odd}. \end{cases} \tag{2.39}$$

- Furthermore, we introduce two parameters $s^1, s^2 = \pm 1$ which describe the winding directions of the exceptional cycles.

Now we are able to write down the final form of the fractional three-cycle which is stemmed from the $\mathbb{Z}_2$-invariant toroidal three-cycle with the wrapping numbers $(m^1, n^1, p^1, 0) \times (\tilde{p}^2, 0, \tilde{p}^2, \tilde{q}^2) \times (m^3, n^3)$. It has the following form:

$$\pi^{\text{frac}} = \frac{1}{2}\pi^{\text{bulk}} + N\frac{\tilde{p}^2\sigma}{2}(s^1\tau^1\gamma_3 + s^2\tau^2\gamma_4) + N\frac{\tilde{q}^2\sigma}{2}(s^1\tau^1\bar{\gamma}_3 + s^2\tau^2\bar{\gamma}_4). \tag{2.40}$$

It is easy to check that the coefficients of π^{bulk}, stemming from the toroidal cycle with the wrapping numbers $(m^1, n^1, p^1, 0) \times (\tilde{p}^2, 0, \tilde{p}^2, \tilde{q}^2) \times (m^3, n^3)$, have N as defined in (2.36) as a common divisor too. Naively one can expect the restriction to $N = 1$ for the co-prime condition. However, this is not necessarily true. Let us for example consider the toroidal cycle with wrapping numbers $(1, 0, -1, 0) \times (0, 0, 0, 1) \times (0, 1)$ passing through the fixed point 1. It gives rise to the fractional cycle $\frac{1}{2}(2\bar{\gamma}_1 \pm 2\bar{\gamma}_3)$. Although $N = 2$ this cycle is co-prime because the cycle $\frac{1}{2}(\bar{\gamma}_1 \pm \bar{\gamma}_3)$ does not exist due to the condition (2.34).

As a consequence of the considerations above we can summarise:

- Any fractional cycle containing only the one-cycle factor $\pi_1 + \pi_3$ ($\tilde{q}^2 = 0$) within the exceptional part can be expressed as a sum over the unbarred cycles γ_i,

$$\pi := v^1 \gamma_1 + v^2 \gamma_2 + v^3 \gamma_3 + v^4 \gamma_4 \,, \tag{2.41}$$

  with an even number of the coefficients v^i with half-integer values.

- Any fractional cycle containing only the one-cycle factor π_4 ($\tilde{p}^2 = 0$) within the exceptional part can be expanded as a sum over the barred cycles $\bar{\gamma}_i$,

$$\bar{\pi} := \bar{v}^1 \bar{\gamma}_1 + \bar{v}^2 \bar{\gamma}_2 - \bar{v}^3 \bar{\gamma}_3 - \bar{v}^4 \bar{\gamma}_4 \,, \tag{2.42}$$

  where $\bar{v}^i$ are either all half-integer or all integer.

In order to determine an integral symplectic basis for the three-cycles, we search for pairs of cycles π and $\bar{\pi}$ such that $\pi \circ \bar{\pi} = -2$, with the coefficients v^i and $\bar{v}^i$ satisfying[3] $\operatorname{sgn} v^i = \operatorname{sgn} \bar{v}^i$ for all i. All possible cycles can be combined in three sets:

1. $(v^1, v^2, v^3, v^4) = (\underline{\pm\frac{1}{2}, \pm\frac{1}{2}, 0, 0})$ and $(\bar{v}^1, \bar{v}^2, \bar{v}^3, \bar{v}^4) = (\underline{\pm 1, \pm 1, 0, 0})$ where the underlying denotes all permutations of entries.

2. $(v^1, v^2, v^3, v^4) = (\underline{\pm 1, 0, 0, 0})$ for the (un-)barred cycles.

3. $(v^1, v^2, v^3, v^4) = (\pm\frac{1}{2}, \pm\frac{1}{2}, \pm\frac{1}{2}, \pm\frac{1}{2})$ for the (un-)barred cycles.

Altogether there are 48 unbarred and 48 barred cycles. It is not difficult to specify a basis of these cycles. For the unbarred part we obtain

$$
\begin{aligned}
\alpha_1 &:= \left(0, \frac{1}{2}, -\frac{1}{2}, 0\right), \\
\alpha_2 &:= \left(0, 0, \frac{1}{2}, -\frac{1}{2}\right), \\
\alpha_3 &:= (0, 0, 0, 1), \\
\alpha_4 &:= \left(\frac{1}{2}, -\frac{1}{2}, -\frac{1}{2}, -\frac{1}{2}\right),
\end{aligned}
\tag{2.43}
$$

---

[3]The signum function is given by

$$
\operatorname{sgn}(x) := \begin{cases} -1 & \text{if } x < 0\,, \\ 0 & \text{if } x = 0\,, \\ 1 & \text{if } x > 0\,. \end{cases}
$$

and for the barred one,

$$\begin{aligned}
\bar{\alpha}_1 &:= (0, 1, 1, 0)\,, \\
\bar{\alpha}_2 &:= (0, 0, -1, 1)\,, \\
\bar{\alpha}_3 &:= (0, 0, 0, -1)\,, \\
\bar{\alpha}_4 &:= \left(\frac{1}{2}, -\frac{1}{2}, \frac{1}{2}, \frac{1}{2}\right).
\end{aligned} \tag{2.44}$$

Therefore, the fractional cycles form the $F_4 \oplus F_4$-lattice, and the intersection matrix takes the form

$$\alpha_i \circ \bar{\alpha}_j = \begin{pmatrix} -2 & 1 & 0 & 0 \\ 1 & -2 & 2 & 0 \\ 0 & 1 & -2 & 1 \\ 0 & 0 & 1 & -2 \end{pmatrix}. \tag{2.45}$$

This is the Cartan matrix for F_4, and it is unimodular. Indeed, it is easy to verify that any bulk, exceptional or fractional cycle can be expanded in the basis (2.43) and (2.44) with integer coefficients. In other words, since the determinant of the intersection matrix (2.45) is 1, the α_i's and $\bar{\alpha}_i$'s form an integral basis of the homology lattice $H_3(M, \mathbb{Z})$.

3 Intersecting brane worlds

The aim of this article is not only the study of non-factorisable $\mathbb{Z}_4$-orbifolds but also model building with $\mathbb{Z}_4$-orientifolds of Type IIA superstring theory. We are interested in global supersymmetric models with a semi-realistic chiral spectrum, in particular Pati-Salam-models as D6-brane realisations with only three visible stacks, which have on other lattices been the most simple kind of global GUT model to be found, see e.g. [31, 34, 40, 46, 48, 87–89]. The introduction of an anti-holomorphic involution $\mathcal{R}$ on the $\mathbb{Z}_4$-orbifold gives rise to orientifold six-planes (O6-planes), which wrap the fixed loci of $\mathcal{R}Q^k$ which together form some element of $H_3(T^6/\mathbb{Z}_4, \mathbb{Z})$. In the following, we denote this homological cycle by π_{O6}. The ($\mathbb{Z}_4$-orbits of) O6-planes have negative RR charge, which has to be canceled by introducing stacks of N_a space-time filling D6-branes which wrap a three-cycle π_a on the orbifold. The RR tadpole cancellation condition is given by [86]

$$\sum_a N_a(\pi_a + \pi'_a) - 4\pi_{\text{O6}} = 0\,, \tag{3.1}$$

where π'_a is the $\mathcal{R}$-image of the three-cycle π_a with in general $\pi'_a \neq \pi_a$. The resulting gauge group is then generically $\prod_a \mathrm{U}(N_a)$. The case $\pi'_a = \pi_a$ gives rise to the rank-preserving symmetry enhancement: $\mathrm{U}(N_a) \hookrightarrow \mathrm{USp}(2N_a)$ or $\mathrm{SO}(2N_a)$. We call a model with the RR tadpole condition (3.1) implemented *global*, otherwise *local*. The chiral massless spectrum can be computed from topological intersection numbers [86]. For the gauge group $\prod_a \mathrm{U}(N_a)$ it is given in the table 2.

Furthermore, the ($\mathbb{Z}_4$-orbits of the) O6-planes preserve $\mathcal{N} = 1$. For semi-realistic models to be supersymmetric, we have to require that all D6-branes preserve the same

Chiral spectrum	
Representation	Multiplicity
$(\mathbf{Sym})_a$	$\frac{1}{2}(\pi_a \circ \pi_a' - \pi_a \circ \pi_{\mathrm{O6}})$
$(\mathbf{Anti})_a$	$\frac{1}{2}(\pi_a \circ \pi_a' + \pi_a \circ \pi_{\mathrm{O6}})$
$(\mathbf{N}_a, \bar{\mathbf{N}}_b)$	$\pi_a \circ \pi_b$
$(\mathbf{N}_a, \mathbf{N}_b)$	$\pi_a \circ \pi_b'$

Table 2. Chiral spectrum for intersecting D6-branes with gauge group $\prod_a \mathrm{U}(N_a)$.

supersymmetry, i.e., that they are wrapped on *special Lagrangian* three-cycles with the same calibration as the O6-planes. These additional constraints on the wrapped three-cycles will be considered in more details in the section 3.2.

3.1 Anti-holomorphic involutions $\mathcal{R}$ of $T^6/\mathbb{Z}_4$

Before we start with the construction of the ($\mathbb{Z}_4$-orbit of) O6-plane(s), we have to calculate how the anti-holomorphic involution acts on the real lattice in each case. It is known [90, 91] that there exist a set of complex coordinates $\{z^i\}_{i=1,2,3}$ on which the twist Q (2.23) acts diagonally

$$Q^t z^i = e^{2\pi i \zeta_i} z^i \tag{3.2}$$

with the eigenvalues $(i, -1, i)$ for the shift vector $\vec{\zeta} = \frac{1}{4}(1, -2, 1)$. In these coordinates, the anti-holomorphic involution (including $\mathbb{Z}_4$-twists) is simply given by complex conjugation

$$\mathcal{R}(Q^t)^n: \quad z^i \to e^{i\theta_{n_i}} \bar{z}^i \tag{3.3}$$

for some real parameter θ_{n_i}. We will now discuss the *a priori* different possible choices of $(\theta_{n_1}, \theta_{n_2}, \theta_{n_3})$ for each $\mathbb{Z}_4$-invariant background lattice and argue that some of the different choices lead to physically equivalent vacua, at least based on the allowed ranks of gauge groups in the RR tadpole cancellation conditions as well as on the counting of supersymmetric bulk cycles per given length.

3.1.1 $B_2 \times (A_1)^2 \times B_2$

In the factorisable case, there exist *a priori* two choices of orientifold axes per two-torus [92–94] denoted by $\mathbf{A}$ (reflection along the short one-cycle, here $\pi_{2/6}$ or some $\mathbb{Z}_4$-images thereof, cf. figure 1) and $\mathbf{B}$ (reflection along the long one-cycle, here $\pi_{1/5}$) for the B_2-tori and two lattice orientations $\mathbf{a}$ (rectangular lattice) and $\mathbf{b}$ (tilted lattice) for the $(A_1)^2$ torus. Due to the permutation symmetry $T_1^2 \leftrightarrow T_3^2$, here the combinatorics provides at most six inequivalent choices of phases (3.3), denoted by $\mathbf{AaA}$, $\mathbf{AaB}$, $\mathbf{BaB}$ and $\mathbf{AbA}$, $\mathbf{AbB}$, $\mathbf{BbB}$, for which the O6-planes are displayed in table 3.

However, the massless closed string spectrum — encoded in the orientifold-even and -odd Hodge numbers $(h_{11}^+, h_{11}^-, h_{21})$ counting vectors, Kähler and complex structure moduli as derived for generic Calabi-Yau backgrounds in [95] —, which was derived using CFT techniques in [34, 45] suggests that there are pairwise relations $\mathbf{AaA} \leftrightarrow \mathbf{BaB}$ and $\mathbf{AbA} \leftrightarrow$

O6-planes on the $B_2 \times (A_1)^2 \times B_2$ lattice			
lattice	**Aa/bA**	**Aa/bB**	**Ba/bB**
$\mathcal{R}$	$8(1-b)\pi_{236}$	$4(1-b)\pi_{235}$	$2(1-b)\pi_{135}$
$\mathcal{R}Q$	$2(\pi_1+2\pi_2)\wedge(\pi_4-b\pi_3)\wedge(\pi_5+2\pi_6)$	$4(\pi_1+2\pi_2)\wedge(b\pi_3-\pi_4)\wedge\pi_6$	$8\pi_2\wedge(\pi_4-b\pi_3)\wedge\pi_6$
$\mathcal{R}Q^2$	$-8(1-b)(\pi_1+\pi_2)\wedge\pi_3\wedge(\pi_5+\pi_6)$	$4(1-b)(\pi_1+\pi_2)\wedge\pi_3\wedge(\pi_5+2\pi_6)$	$-2(1-b)(\pi_1+2\pi_2)\wedge\pi_3\wedge(\pi_5+2\pi_6)$
$\mathcal{R}Q^3$	$2\pi_1\wedge(b\pi_3-\pi_4)\wedge\pi_5$	$4\pi_1\wedge(\pi_4-b\pi_3)\wedge(\pi_5+\pi_6)$	$8(\pi_1+\pi_2)\wedge(b\pi_3-\pi_4)\wedge(\pi_5+\pi_6)$

Table 3. Fixed planes for the different lattice orientations of $B_2 \times (A_1)^2 \times B_2$, weighted with the number $N_{O6} = 2(1 - b)$ of parallel O6-planes along T_2^2 with $b = 0, \frac{1}{2}$ for **a** and **b**, respectively.

BbB, reducing the number of physically inequivalent backgrounds to four. This assumption is supported by the analogy to the relations among different lattice backgrounds derived for $\mathbb{Z}_6^{(\prime)}$ and $\mathbb{Z}_2 \times \mathbb{Z}_6^{(\prime)}$ in [42, 46, 48].

Since D6-branes on the factorisable $T^6/(\mathbb{Z}_4 \times \Omega\mathcal{R})$ orientifold have been considered at length in [34] with the result that at most two generations of chiral particles can be engineered by two supersymmetric intersecting D6-brane orbits, we will from now on concentrate on backgrounds with non-factorisable tori, where we will determine all *a priori* different choices of lattice orientations and then search for physical equivalences.

3.1.2 $A_3 \times A_3$

The eigenvectors of Q^t with Q defined in (2.12) give rise to the complex coordinates [84]

$$
\begin{aligned}
z^1 &:= \frac{1}{\sqrt{2}}(x^1 + ix^2 - x^3)\,, \\
z^2 &:= \frac{1}{\sqrt{8u_2}}\big((x^1 - x^2 + x^3 + \mathcal{U}(x^4 - x^5 + x^6))\big)\,, \\
z^3 &:= \frac{1}{\sqrt{2}}(x^4 + ix^5 - x^6)\,,
\end{aligned}
\tag{3.4}
$$

where the complex structure is $\mathcal{U} := u_1 + iu_2 = -\frac{R_2}{2aR_1}\big(c + e + i\sqrt{-(c+e)^2 + 4ab}\big)$.

With the transformation from the complex coordinates to the real ones, we are able to write down the action of $\mathcal{R}$ on the real lattice. There are *a priori* four possible choices of angles in the anti-holomorphic involution:

$$
\vec{\theta} = (0,0,0) \Rightarrow \left\{ \begin{array}{ll} \mathcal{R}_1 e_1 = e_1\,, & \mathcal{R}_1 e_2 = -e_1 - e_2 - e_3\,, \\ \mathcal{R}_1 e_3 = e_3\,, & \mathcal{R}_1 e_4 = u_1(e_1 + e_3) - e_6\,, \\ \mathcal{R}_1 e_5 = -u_1(e_1 + e_3) - e_5\,, & \mathcal{R}_1 e_6 = u_1(e_1 + e_3) - e_4\,, \end{array} \right\} \quad \mathbf{AAA} \tag{3.5}
$$

$$
\vec{\theta} = \left(\frac{\pi}{2},0,0\right) \Rightarrow \left\{ \begin{array}{ll} \mathcal{R}_2 e_1 = e_1 + e_2 + e_3\,, & \mathcal{R}_2 e_2 = -e_3\,, \\ \mathcal{R}_2 e_3 = -e_2\,, & \mathcal{R}_1 e_4 = u_1(e_1 + e_3) - e_6\,, \\ \mathcal{R}_1 e_5 = -u_1(e_1 + e_3) - e_5\,, & \mathcal{R}_1 e_6 = u_1(e_1 + e_3) - e_4\,, \end{array} \right\} \quad \mathbf{BAA} \tag{3.6}
$$

$$
\vec{\theta} = \left(0,0,\frac{\pi}{2}\right) \Rightarrow \left\{ \begin{array}{ll} \mathcal{R}_3 e_1 = e_1\,, & \mathcal{R}_3 e_2 = -e_1 - e_2 - e_3\,, \\ \mathcal{R}_3 e_3 = e_3\,, & \mathcal{R}_3 e_4 = u_1(e_1 + e_3) + e_5\,, \\ \mathcal{R}_3 e_5 = u_1(e_1 + e_3) + e_4\,, & \mathcal{R}_3 e_6 = u_1(e_1 + e_3) - e_4 - e_5 - e_6\,, \end{array} \right\} \quad \mathbf{AAB}
$$

$$
\tag{3.7}
$$

O6-planes for AAA-lattice of $A_3 \times A_3$-orbifold	
Projection	Fixed point set
$\mathcal{R}_1$	$2(\pi_{134} - \pi_{136})$
$\mathcal{R}_1 Q$	$2(\pi_{245} + \pi_{246} - \pi_{256} + \pi_{345} + \pi_{346} - \pi_{356})$
$\mathcal{R}_1 Q^2$	$2(\pi_{124} + 2\pi_{125} + \pi_{126} - \pi_{234} - 2\pi_{235} - \pi_{236})$
$\mathcal{R}_1 Q^3$	$2(-\pi_{145} + \pi_{146} + \pi_{156} - \pi_{245} + \pi_{246} + \pi_{256})$

Table 4. Toroidal cycles wrapped by the O6-planes on the **AAA** lattice orientation of $A_3 \times A_3$.

$$\vec{\theta} = \left(\frac{\pi}{2}, 0, \frac{\pi}{2}\right) \Rightarrow \left\{ \begin{array}{ll} \mathcal{R}_4 e_1 = e_1 + e_2 + e_3\,, & \mathcal{R}_4 e_2 = -e_3\,, \\ \mathcal{R}_4 e_3 = -e_2\,, & \mathcal{R}_4 e_4 = u_1(e_1 + e_3) + e_5\,, \\ \mathcal{R}_4 e_5 = u_1(e_1 + e_3) + e_4\,, & \mathcal{R}_4 e_6 = u_1(e_1 + e_3) - e_4 - e_5 - e_6\,. \end{array} \right\} \quad \textbf{BAB}$$

(3.8)

Here we took the notation for the lattices from [63], which we will now explain. The complex coordinates (3.4) parametrise the three-planes[4] where Q acts as a rotation. **A** means that, in their choice of basis, the orientifold plane lies along the horizontal axis in the corresponding plane, while **B** corresponds to the angle of the orientifold plane with respect to the horizontal axis being $\pi/4$.

Note also that in contrast to the $B_2 \times (A_1)^2 \times B_2$-orbifold, the **BAA**- and **AAB**-lattices are really different geometrically and cannot be related by exchanging $T_1^3 \leftrightarrow T_2^3$. This will be further specified in the sections 3.3 and 4.

Since only a crystallographic action on the lattice is allowed ($\mathcal{R}_i r = r + \Lambda$ for arbitrary lattice vectors $r \in \Lambda$), the real part of the complex structure can take only the value $u_1 = 0$ ($\Rightarrow c + e = 0$ in (2.13) and only **A** as middle entry of the lattice orientation). The orientifold projections act then on the homology classes of three-cycles (2.15) in the following way:

$$\mathcal{R}_1: \qquad \gamma_1 \leftrightarrow -\gamma_2\,, \qquad \bar{\gamma}_1 \leftrightarrow \bar{\gamma}_2\,.$$

(3.9)

$$\mathcal{R}_{2/3}: \qquad \begin{cases} \gamma_1 \to \gamma_1\,, & \bar{\gamma}_1 \to -\bar{\gamma}_1\,, \\ \gamma_2 \to -\gamma_2\,, & \bar{\gamma}_2 \to \bar{\gamma}_2\,. \end{cases}$$

(3.10)

$$\mathcal{R}_4: \qquad \gamma_1 \leftrightarrow \gamma_2\,, \qquad \bar{\gamma}_1 \leftrightarrow -\bar{\gamma}_2\,.$$

(3.11)

Furthermore, we calculate the fixed point set for the orientifold involutions $\{\mathcal{R}_i\,, \mathcal{R}_i Q\,, \mathcal{R}_i Q^2\,, \mathcal{R}_i Q^3\}$. The results are listed in tables 4–7 for the respective $\mathcal{R}_i$.

The fixed point set under $\mathcal{R}_i Q^n$ is computed in the following way, e.g. for $\mathcal{R}_1$: first, we calculate the three eigenvectors of $\mathcal{R}_1$ corresponding to the eigenvalue 1, in this case e_1, e_3 and $e_4 - e_6$. The to these vectors corresponding one-cycles π_i span a three-cycle $\pi_{134} - \pi_{136}$. The next step is to determine how many three-cycles of the same homology class we have which are point-wise $\mathcal{R}_1$-invariant. In the case at hand, we obtain two such submanifolds, which go through the $\mathcal{R}_1$ fixed points $(0, 0, 0, 0, \frac{m}{2}, 0)$ with $m \in \{0, 1\}$. The projection $\mathcal{R}_1 Q$ leads to similar results. The fixed point sets of $\mathcal{R} Q^2$ and $\mathcal{R} Q^3$ can be calculated by acting

---

[4]These three-planes are closely related to the "factorisation" of the non-factorisable torus we will discuss in the next section.

O6-planes for BAA-lattice of $A_3 \times A_3$-orbifold	
Projection	Fixed point set
$\mathcal{R}_2$	$2(-\pi_{124} + \pi_{126} + \pi_{134} - \pi_{136} + \pi_{234} - \pi_{236})$
$\mathcal{R}_2 Q$	$2(-\pi_{145} - \pi_{146} + \pi_{156} + \pi_{345} + \pi_{346} - \pi_{356})$
$\mathcal{R}_2 Q^2$	$2(\pi_{124} + 2\pi_{125} + \pi_{126} + \pi_{134} + 2\pi_{135} + \pi_{136} - \pi_{234} - 2\pi_{235} - \pi_{236})$
$\mathcal{R}_2 Q^3$	$2(-\pi_{145} + \pi_{146} + \pi_{156} - 2\pi_{245} + 2\pi_{246} + 2\pi_{256} - \pi_{345} + \pi_{346} + \pi_{356})$

Table 5. Toroidal cycles wrapped by the O6-planes for the **BAA** lattice orientation of $A_3 \times A_3$.

O6-planes for AAB-lattice of $A_3 \times A_3$-orbifold	
Projection	Fixed point set
$\mathcal{R}_3$	$2(\pi_{134} + \pi_{135})$
$\mathcal{R}_3 Q$	$2(\pi_{246} + \pi_{346})$
$\mathcal{R}_3 Q^2$	$2(\pi_{125} + \pi_{126} - \pi_{235} - \pi_{236})$
$\mathcal{R}_3 Q^3$	$2(-\pi_{145} + \pi_{156} - \pi_{245} + \pi_{256})$

Table 6. Toroidal cycles wrapped by the O6-planes for the **AAB** lattice orientation of $A_3 \times A_3$.

O6-planes for BAB-lattice of $A_3 \times A_3$-orbifold	
Projection	Fixed point set
$\mathcal{R}_4$	$2(-\pi_{124} - \pi_{125} + \pi_{134} + \pi_{135} + \pi_{234} + \pi_{235})$
$\mathcal{R}_4 Q$	$2(\pi_{146} - \pi_{346})$
$\mathcal{R}_4 Q^2$	$2(\pi_{125} + \pi_{126} + \pi_{135} + \pi_{136} - \pi_{235} - \pi_{236})$
$\mathcal{R}_4 Q^3$	$2(\pi_{145} - \pi_{156} + 2\pi_{245} - 2\pi_{256} + \pi_{345} - \pi_{356})$

Table 7. Toroidal cycles wrapped by the O6-planes for the **BAB** lattice orientation of $A_3 \times A_3$.

with Q on the $\mathcal{R}$- and $\mathcal{R}Q$-fixed point sets, respectively. After all fixed point sets have been computed, from purely geometric considerations there still remains an ambiguity in both the global sign of all sets and the relative sign between the $\mathcal{R}$- and $\mathcal{R}Q$-sets which needs to be fixed, i.e., the three-cycle $\pm\big(\mathrm{Fix}(\mathcal{R} + \mathcal{R}Q^2) \pm \mathrm{Fix}(\mathcal{R}Q + \mathcal{R}Q^3)\big)$ is invariant for any choice of the signs. Each of the two sets of fixed points corresponds to a different bulk cycle. Asking both of them to have the same calibration will fix the relative sign between them. The global sign is fixed once we choose one of the two possible calibration conditions (either $\int(e^{i\varphi}\Omega_3) > 0$ or $\int(e^{i\varphi+i\pi}\Omega_3) > 0$); alternatively, choosing the global sign will fix the calibration condition that has to be used. This calibration will be explained in more detail in section 3.2.

Adding all contributions, we can express the corresponding O6-planes as elements of $H_3(T^6/\mathbb{Z}_4, \mathbb{Z})$:

$$\pi_{\mathrm{O6}_1} := 2(\gamma_2 - \gamma_1) - 2(\bar{\gamma}_1 + \bar{\gamma}_2)\,, \tag{3.12a}$$

$$\pi_{\mathrm{O6}_2} := -4\gamma_1 - 4\bar{\gamma}_2\,, \tag{3.12b}$$

$$\pi_{\mathrm{O6}_3} := -2\gamma_1 - 2\bar{\gamma}_2\,, \tag{3.12c}$$

$$\pi_{\mathrm{O6}_4} := 2(\gamma_1 + \gamma_2) + 2(\bar{\gamma}_2 - \bar{\gamma}_1)\,. \tag{3.12d}$$

Obviously, the O6-planes (3.12) are invariant under the corresponding orientifold projections given in equations (3.9), (3.10) and (3.11).

3.1.3 $A_3 \times A_1 \times B_2$

We can approach the $A_3 \times A_1 \times B_2$-case in an analogous way. Due to (3.2), the complex coordinates are:

$$
\begin{aligned}
z^1 &= \frac{1}{\sqrt{2}}(x^1 + ix^2 - x^3)\,, \\
z^2 &= \frac{1}{2\sqrt{2\,\mathrm{Im}(\mathcal{U})}}(x^1 - x^2 + x^3 + 2\mathcal{U}x^4)\,, \\
z^3 &= x^5 - \frac{x^6}{2} + i\frac{x^6}{2}\,,
\end{aligned}
\tag{3.13}
$$

with the complex structure

$$\mathcal{U} := u_1 + iu_2 := -\frac{R_1}{2aR_3}\big(d + i\sqrt{-a - d^2}\big)\,. \tag{3.14}$$

For this non-factorisable lattice, there are four possible orientations:

$$\vec{\theta} = (0,0,0) \Rightarrow \left\{ \begin{array}{ll} \mathcal{R}_1 e_1 = e_1\,, & \mathcal{R}_1 e_2 = -e_1 - e_2 - e_3\,, \\ \mathcal{R}_1 e_3 = e_3\,, & \mathcal{R}_1 e_4 = 2u_1(e_1 + e_3) - e_4\,, \\ \mathcal{R}_1 e_5 = e_5\,, & \mathcal{R}_1 e_6 = -e_5 - e_6\,, \end{array} \right\} \quad \mathbf{AAB} \tag{3.15}$$

$$\vec{\theta} = \left(0,0,-\frac{\pi}{2}\right) \Rightarrow \left\{ \begin{array}{ll} \mathcal{R}_2 e_1 = e_1\,, & \mathcal{R}_2 e_2 = -e_1 - e_2 - e_3\,, \\ \mathcal{R}_2 e_3 = e_3\,, & \mathcal{R}_2 e_4 = 2u_1(e_1 + e_3) - e_4\,, \\ \mathcal{R}_2 e_5 = -e_5 - 2e_6\,, & \mathcal{R}_2 e_6 = e_6\,, \end{array} \right\} \quad \mathbf{AAA} \tag{3.16}$$

$$\vec{\theta} = \left(-\frac{\pi}{2},0,-\frac{\pi}{2}\right) \Rightarrow \left\{ \begin{array}{ll} \mathcal{R}_3 e_1 = -e_2\,, & \mathcal{R}_3 e_2 = -e_1\,, \\ \mathcal{R}_3 e_3 = e_1 + e_2 + e_3\,, & \mathcal{R}_3 e_4 = 2u_1(e_1 + e_3) - e_4\,, \\ \mathcal{R}_3 e_5 = -e_5 - 2e_6\,, & \mathcal{R}_3 e_6 = e_6\,, \end{array} \right\} \quad \mathbf{ABA} \tag{3.17}$$

and

$$\vec{\theta} = \left(-\frac{\pi}{2},0,0\right) \Rightarrow \left\{ \begin{array}{ll} \mathcal{R}_4 e_1 = -e_2\,, & \mathcal{R}_4 e_2 = -e_1\,, \\ \mathcal{R}_4 e_3 = e_1 + e_2 + e_3\,, & \mathcal{R}_4 e_4 = 2u_1(e_1 + e_3) - e_4\,, \\ \mathcal{R}_4 e_5 = e_5\,, & \mathcal{R}_4 e_6 = -e_5 - e_6\,. \end{array} \right\} \quad \mathbf{ABB} \tag{3.18}$$

Here we also took again the notation for the lattices from [63]. Since only the crystallographic action on the lattice is allowed ($\mathcal{R}_i r = r + \Lambda$ for arbitrary lattice vectors $r \in \Lambda$), the real part of the complex structure can take only two values $u_1 = 0, \frac{1}{2}$. We adapt the above lattice notation for different values of u_1 in the following way: we write a small **a**

O6-planes for AAB-lattice of $A_3 \times A_1 \times B_2$-orbifold	
Projection	Fixed point set
$\mathcal{R}_1$	$2\pi_{135}$
$\mathcal{R}_1 Q$	$4\big(u_1(\pi_{126} + \pi_{136} - \pi_{236}) + \pi_{246} + \pi_{346}\big)$
$\mathcal{R}_1 Q^2$	$2\pi_{125} + 4\pi_{126} - 2\pi_{235} - 4\pi_{236}$
$\mathcal{R}_1 Q^3$	$4\big(u_1(\pi_{135} + \pi_{136} - \pi_{125} - \pi_{126} + \pi_{235} + \pi_{236}) - \pi_{145} - \pi_{146} - \pi_{245} - \pi_{246}\big)$

Table 8. Toroidal cycles wrapped by the O6-planes for the **AAB** orientation of $A_3 \times A_1 \times B_2$.

and **b** as a subscript after the first **A** for $u_1 = 0$ and $u_1 = \frac{1}{2}$, respectively. The **b**-type lattice is to our best knowledge investigated here for the first time, while the D6-brane configurations, which cancel the bulk RR tadpoles locally on top of the O6-planes, in [63] correspond to the **a**-type choice $u_1 = 0$.

The orientifold action on the homological three-cycles is given by

$$
\mathcal{R}_1 : \begin{cases}
\gamma_1 \to \gamma_2\,, & \bar{\gamma}_1 \to -\bar{\gamma}_2 - 2u_1\gamma_2\,, \\
\gamma_2 \to \gamma_1\,, & \bar{\gamma}_2 \to -\bar{\gamma}_1 - 2u_1\gamma_1\,, \\
\gamma_3 \to \gamma_3\,, & \bar{\gamma}_3 \to -\bar{\gamma}_3 + 2u_1\gamma_3\,, \\
\gamma_4 \to \gamma_4\,, & \bar{\gamma}_4 \to -\bar{\gamma}_4 + 2u_1\gamma_4\,.
\end{cases}
\tag{3.19}
$$

$$
\mathcal{R}_2 : \begin{cases}
\gamma_1 \to \gamma_1\,, & \bar{\gamma}_1 \to -\bar{\gamma}_1 - 2u_1\gamma_1\,, \\
\gamma_2 \to -\gamma_2\,, & \bar{\gamma}_2 \to \bar{\gamma}_2 + 2u_1\gamma_2\,, \\
\gamma_3 \to -\gamma_3\,, & \bar{\gamma}_3 \to \bar{\gamma}_3 - 2u_1\gamma_3\,, \\
\gamma_4 \to -\gamma_4\,, & \bar{\gamma}_4 \to \bar{\gamma}_4 - 2u_1\gamma_4\,.
\end{cases}
\tag{3.20}
$$

$$
\mathcal{R}_3 : \begin{cases}
\gamma_1 \to -\gamma_2\,, & \bar{\gamma}_1 \to \bar{\gamma}_2 + 2u_1\gamma_2\,, \\
\gamma_2 \to -\gamma_1\,, & \bar{\gamma}_2 \to \bar{\gamma}_1 + 2u_1\gamma_1\,, \\
\gamma_3 \to -\gamma_3\,, & \bar{\gamma}_3 \to \bar{\gamma}_3 - 2u_1\gamma_3\,, \\
\gamma_4 \to -\gamma_4\,, & \bar{\gamma}_4 \to \bar{\gamma}_4 - 2u_1\gamma_4\,.
\end{cases}
\tag{3.21}
$$

$$
\mathcal{R}_4 : \begin{cases}
\gamma_1 \to \gamma_1\,, & \bar{\gamma}_1 \to -\bar{\gamma}_1 - 2u_1\gamma_1\,, \\
\gamma_2 \to -\gamma_2\,, & \bar{\gamma}_2 \to \bar{\gamma}_2 + 2u_1\gamma_2\,, \\
\gamma_3 \to \gamma_3\,, & \bar{\gamma}_3 \to -\bar{\gamma}_3 + 2u_1\gamma_3\,, \\
\gamma_4 \to \gamma_4\,, & \bar{\gamma}_4 \to -\bar{\gamma}_4 + 2u_1\gamma_4\,.
\end{cases}
\tag{3.22}
$$

Furthermore, we can calculate the fixed point sets for the orientifold projections $\{\mathcal{R}_i\,, \mathcal{R}_i Q\,, \mathcal{R}_i Q^2\,, \mathcal{R}_i Q^3\}$. The results are listed in tables 8–11 for the respective $\mathcal{R}_i$. In figures 4–8 we illustrate the O6-planes for the lattices $\mathbf{A_a AB}$ and $\mathbf{A_a BB}$.[5]

---

[5]We will see in the next section that the other **a**-type lattices are related to these.

O6-planes for AAA-lattice of $A_3 \times A_1 \times B_2$-orbifold	
Projection	Fixed point set
$\mathcal{R}_2$	$4\pi_{136}$
$\mathcal{R}_2 Q$	$2\Big(-u_1\big(\pi_{125} + \pi_{135} - \pi_{235} + 2(\pi_{126}+\pi_{136}-\pi_{236})\big) - \pi_{245} - \pi_{345} - 2(\pi_{246}+\pi_{346})\Big)$
$\mathcal{R}_2 Q^2$	$4(-\pi_{125} - \pi_{126} + \pi_{235} + \pi_{236})$
$\mathcal{R}_2 Q^3$	$2\big(-u_1(\pi_{135} - \pi_{125} + \pi_{235}) - \pi_{145} - \pi_{245}\big)$

Table 9. Toroidal cycles wrapped by the O6-planes for the **AAA** orientation of $A_3 \times A_1 \times B_2$.

O6-planes for ABA-lattice of $A_3 \times A_1 \times B_2$-orbifold	
Projection	Fixed point set
$\mathcal{R}_3$	$(4 - 4u_1)(\pi_{126} + \pi_{136} - \pi_{236})$
$\mathcal{R}_3 Q$	$2\big(-2u_1(\pi_{125} - \pi_{235} + 2\pi_{126} - 2\pi_{236}) - \pi_{145} - 2\pi_{245} - \pi_{345} - 2(\pi_{146} + 2\pi_{246} + \pi_{346})\big)$
$\mathcal{R}_3 Q^2$	$(4 - 4u_1)(-\pi_{125} - \pi_{126} + \pi_{135} + \pi_{136} + \pi_{235} + \pi_{236})$
$\mathcal{R}_3 Q^3$	$2(-2u_1\pi_{135} + \pi_{145} - \pi_{345})$

Table 10. Toroidal cycles wrapped by the O6-planes for the **ABA** orientation of $A_3 \times A_1 \times B_2$.

O6-planes for ABB-lattice of $A_3 \times A_1 \times B_2$-orbifold	
Projection	Fixed point set
$\mathcal{R}_4$	$(2 - 2u_1)(\pi_{125} + \pi_{135} - \pi_{235})$
$\mathcal{R}_4 Q$	$4\big(2u_1(\pi_{126} - \pi_{236}) + \pi_{146} + 2\pi_{246} + \pi_{346}\big)$
$\mathcal{R}_4 Q^2$	$(2 - 2u_1)(\pi_{125} + 2\pi_{126} - \pi_{135} - 2\pi_{136} - \pi_{235} - 2\pi_{236})$
$\mathcal{R}_4 Q^3$	$4\big(2u_1(\pi_{135} + \pi_{136}) - \pi_{145} - \pi_{146} + \pi_{345} + \pi_{346}\big)$

Table 11. Toroidal cycles wrapped by the O6-planes for the **ABB** orientation of $A_3 \times A_1 \times B_2$.
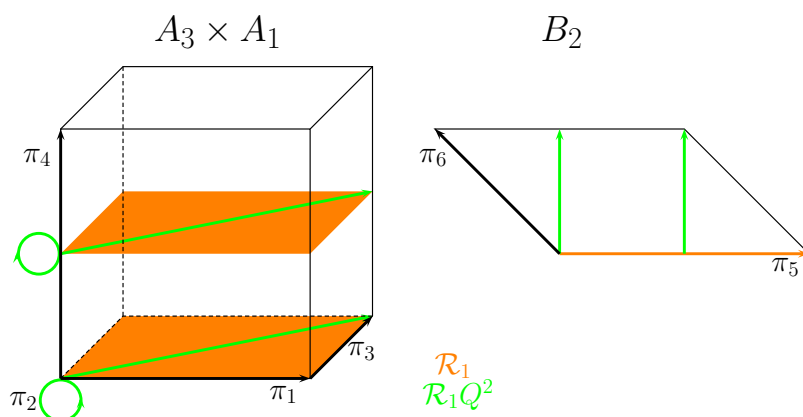

Figure 4. $\mathcal{R}_1$- and $\mathcal{R}_1 Q^2$-contributions to the O6-planes of the $A_3 \times A_1 \times B_2$-orientifold with **A$_\mathbf{a}$AB**-lattice ($u_1 = 0$).

Figure 5. $\mathcal{R}_1 Q$- and $\mathcal{R}_1 Q^3$-contributions to the O6-plane of the $A_3 \times A_1 \times B_2$-orientifold with **$A_a AB$**-lattice ($u_1 = 0$).
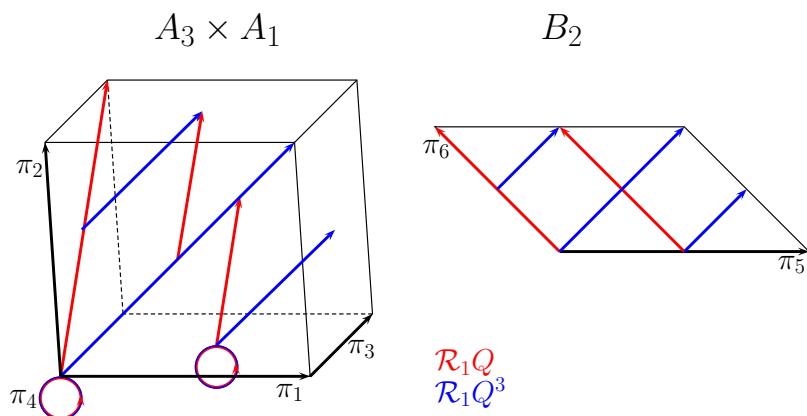

Figure 6. $\mathcal{R}_4$-contribution to the O6-plane of the $A_3 \times A_1 \times B_2$-orientifold with **$A_a BB$**-lattice ($u_1 = 0$). The second fixed point set is located at $\pi_4 = \frac{1}{2}$ and denoted by the orange point in the picture.

Adding up all contributions we obtain the corresponding O6-planes:

$$\pi_{O6_1} := (1 - 2u_1)\gamma_1 + (1 + 2u_1)\gamma_2 - 2(\bar{\gamma}_1 - \bar{\gamma}_2) \,, \tag{3.23a}$$

$$\pi_{O6_2} := -2\gamma_1 - 2u_1\gamma_2 - 2\bar{\gamma}_2 \,, \tag{3.23b}$$

$$\pi_{O6_3} := 2(\gamma_2 - \gamma_1) - 4u_1\gamma_2 - 2(\bar{\gamma}_1 + \bar{\gamma}_2) \,, \tag{3.23c}$$

$$\pi_{O6_4} := (2 - 2u_1)\gamma_1 + 4u_1\gamma_2 + 4\bar{\gamma}_2 \,. \tag{3.23d}$$

It is easy to check that the resulting O6-planes are invariant under corresponding orientifold projections defined in equations (3.19) to (3.22).

3.2 Supersymmetric cycles

From the phenomenological point of view (like chirality and stability at low energies) $\mathcal{N} = 1$ supersymmetric models are particularly interesting. This requires the D6-branes

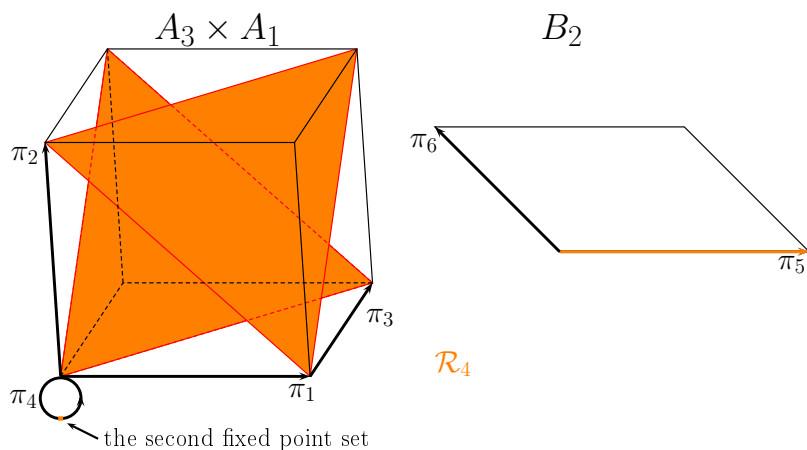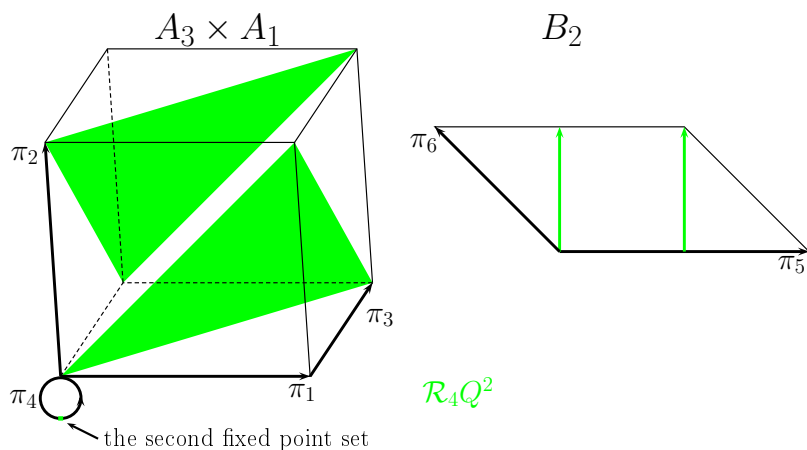**Figure 7**. $\mathcal{R}_4 Q^2$-contributions to the O6-plane of the $A_3 \times A_1 \times B_2$-orientifold with $\mathbf{A_a BB}$-lattice ($u_1 = 0$). The second fixed point set is located at $\pi_4 = \frac{1}{2}$ and denoted by the green point in the picture.
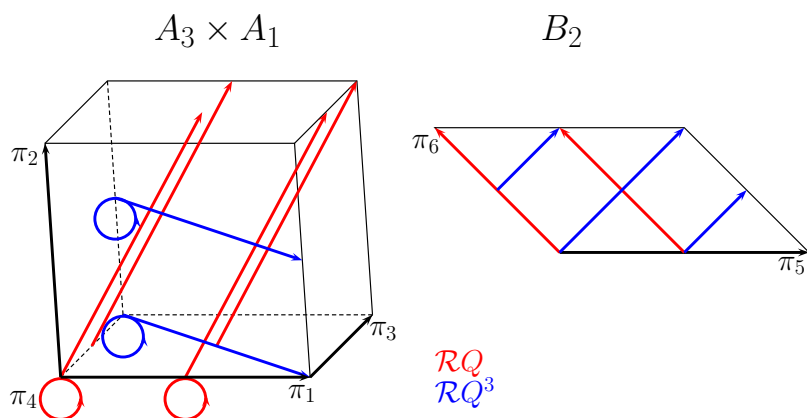

Figure 8. $\mathcal{R}_4 Q$- and $\mathcal{R}_4 Q^3$-contributions to the O6-plane of the $A_3 \times A_1 \times B_2$-orientifold with $\mathbf{A_a BB}$-lattice ($u_1 = 0$).

to preserve some supersymmetry, which leads to additional geometrical conditions on the allowed three-cycles; namely, the three-cycles have to be special Lagrangian. A three-cycle π is called special Lagrangian ($sLag$) if it satisfies

$$J \mid_\pi = 0 \,, \tag{3.24a}$$

$$\mathrm{Im}(e^{i\varphi}\Omega_3) \mid_\pi = 0 \,, \tag{3.24b}$$

$$\mathrm{Re}(e^{i\varphi}\Omega_3) \mid_\pi > 0 \,, \tag{3.24c}$$

where φ is an arbitrary constant phase, and J and Ω_3 are the covariantly constant Kähler two-form and holomorphic three-form, respectively, that always exist on a Calabi-Yau threefold (and, in particular, on the $T^6/\mathbb{Z}_4$ orbifold we consider here). They can be defined

locally by

$$\Omega_3 = dz^1 \wedge dz^2 \wedge dz^3, \qquad J = i \sum_{i,\bar{j}} g_{i\bar{j}} dz^i \wedge d\bar{z}^{\bar{j}}. \tag{3.25}$$

If two Lagrangian three-cycles are calibrated by different values of the phase φ, the corresponding D6-branes preserve different supersymmetries. Since the three-cycle wrapped by the O6-plane is automatically $sLag$, the phase φ is fixed to $\varphi = \varphi_{\mathrm{O6}}$, and we need to search for the Lagrangian three-cycles which are calibrated by $\mathrm{Re}(e^{i\varphi_{\mathrm{O6}}}\Omega_3)$.

In terms of the $\vec{\theta}$, the angle φ_{O6} is given by

$$\varphi_{\mathrm{O6}} = -\frac{1}{2} \sum_i \theta_i \, (+\pi). \tag{3.26}$$

The possible $+\pi$ in the previous equation arises from the freedom we have to choose either $\int(e^{i\varphi}\Omega_3) > 0$ or $\int(e^{i\varphi+i\pi}\Omega_3) > 0$ as the calibration condition, or, alternatively, the global sign of the three-cycle wrapped by the O6-plane.

$B_2 \times (A_1)^2 \times B_2$. Due to the factorisable structure of the $B_2 \times (A_1)^2 \times B_2$-lattice, any three-cycle with the wrapping numbers $(n^i, m^i)_{i=1,2,3}$ is automatically Lagrangian. The condition that a D6-brane wrapping such a three-cycle preserves the same supersymmetry as the O6-plane (i.e. is $sLag$ with identical calibration) is

$$\sum_i \phi_i = 0 \bmod 2\pi \tag{3.27}$$

where ϕ_i is an angle between the three-cycle and the O6-plane on the two-torus $T^2_{(i)}$. Fractional three-cycles with the same calibration arise when (fractions of) exceptional three-cycles are added through which a given bulk cycle passes with the one restriction on the relative prefactor discussed below equation (2.10); for more details see [34].

$A_3 \times A_3$. With respect to the complex coordinates (3.4), the Q-invariant metric g of equation (2.13) is given by

$$g_{i\bar{j}} = \begin{pmatrix} 2R_1^2(1+a) & 0 & R_1 R_2\big(e - c - i(c + 2d + e)\big) \\ 0 & -8u_2 a R_1^2 & 0 \\ R_1 R_2\big(e - c + i(c + 2d + e)\big) & 0 & 2R_2^2(1+b) \end{pmatrix}. \tag{3.28}$$

The Kähler-form J on the $A_3 \times A_3$-lattice background is given by

$$J := 2R_1^2(1+a)\omega_1 - 2u_2 a R_1^2 \omega_2 + 2R_2^2(1+b)\omega_3 + R_1 R_2\big((c + 2d + e)\omega_4 + (c - e)\omega_5\big) \tag{3.29}$$

with real $\mathbb{Z}_4$-invariant two-forms ω_i:

$$\begin{aligned}
\omega_1 &:= dx^{12} + dx^{23}, \\
\omega_2 &:= dx^{14} - dx^{15} + dx^{16} - dx^{24} + dx^{25} - dx^{26} + dx^{34} - dx^{35} + dx^{36}, \\
\omega_3 &:= dx^{45} + dx^{56}, \\
\omega_4 &:= dx^{14} - dx^{16} + dx^{25} - dx^{34} + dx^{36}, \\
\omega_5 &:= -dx^{15} + dx^{24} - dx^{26} + dx^{35},
\end{aligned} \tag{3.30}$$

where $dx^{ij} := dx^i \wedge dx^j$.

$A_3 \times A_3$-orientifolds				
Lattice	Involution	Invariant part of J	Moduli fixing	φ_{O6_i}
AAA	$\mathcal{R}_1$	ω_4	$d = 0$	0
BAA	$\mathcal{R}_2$	$\omega_4 + \omega_5$	$e = d$	$-\frac{\pi}{4}$
AAB	$\mathcal{R}_3$	$\omega_4 - \omega_5$	$e = -d$	$-\frac{\pi}{4}$
BAB	$\mathcal{R}_4$	ω_4	$d = 0$	$\frac{\pi}{2}$

Table 12. Additional moduli fixing and calibration arising from the condition $\mathcal{R}J = -J$ for the different choices of $A_3 \times A_3$ lattice orientations.

The Kähler two-form is negative under the orientifold projection, i.e. $\mathcal{R}J = -J$. This means that the $\mathcal{R}$-even part of J has to vanish, which fixes part of the moduli, in addition to the fixing $u_1 = 0$ (i.e. $c + e = 0$) mentioned in the previous subsection. The additional moduli fixing for the different orientifold projections is given in table 12.

While, in the factorisable case, i.e. $T^6 = (T^2)^3$, all factorised three-cycles are Lagrangian, this does not hold true anymore on the orbifolds with some non-factorisable lattice. However, if we fix the moduli $c = d = e = 0$, i.e. both A_3-tori are orthogonal to each other, and use the relation $dx^i(\pi_j) = \delta^i_j$, we can verify that any toroidal $\mathbb{Z}_2$-invariant three-cycle (2.22) is automatically Lagrangian.

The next step is to specify the *sLag* condition on our orientifolds $T^6/(\mathbb{Z}_4 \times \Omega\mathcal{R}_i)$ in order to find the supersymmetric three-cycles. The holomorphic three-form $\Omega_3 = \text{Re}\,\Omega_3 + i\,\text{Im}\,\Omega_3$ has the decomposition

$$\text{Re}(\Omega_3) = \frac{1}{8\sqrt{u_2}}(\rho_1 - u_2\rho_4)\,,$$
$$\text{Im}(\Omega_3) = \frac{1}{8\sqrt{u_2}}(\rho_2 + u_2\rho_3)\,,$$

(3.31)

with real $\mathbb{Z}_4$-invariant three-forms

$$
\begin{aligned}
\rho_1 &:= -dx^{124} + dx^{125} + dx^{126} + 2dx^{134} - 2dx^{136} - dx^{234} - dx^{235} + dx^{236}, \\
\rho_2 &:= -dx^{124} - dx^{125} + dx^{126} + 2dx^{135} + dx^{234} - dx^{235} - dx^{236}, \\
\rho_3 &:= dx^{145} - 2dx^{146} + dx^{156} - dx^{245} + dx^{256} - dx^{345} + 2dx^{346} - dx^{356}, \\
\rho_4 &:= dx^{145} - dx^{156} + dx^{245} - 2dx^{246} + dx^{256} - dx^{345} + dx^{356}.
\end{aligned}
$$

(3.32)

Because this case is not so interesting from the phenomenological point of view, we do not go into detail here and only give the supersymmetry parameters φ_{O6_i} in table 12 for each involution.

$A_3 \times A_1 \times B_2$. With respect to the complex coordinates (3.13), the $A_3 \times A_1 \times B_2$-orbifold has the hermitian metric

$$g_{i\bar{j}} = \begin{pmatrix} 2R_3^2(1+a) & 0 & \frac{R_2R_3}{\sqrt{2}}\big(b + i(b+2c)\big) \\ 0 & -8u_2aR_3^2 & 0 \\ \frac{R_2R_3}{\sqrt{2}}\big(b - i(b+2c)\big) & 0 & 2R_2^2 \end{pmatrix}\,,$$

(3.33)

$A_3 \times A_1 \times B_2$-*orientifolds*				
Lattice	Involution	Invariant part of J	Moduli fixing	φ_{O6_i}
AAB	$\mathcal{R}_1$	ω_4	$b = -2c$	0
AAA	$\mathcal{R}_2$	$\omega_4 + \omega_5$	$b = -c$	$\frac{5\pi}{4}$
ABA	$\mathcal{R}_3$	ω_4	$b = -2c$	$\frac{3\pi}{2}$
ABB	$\mathcal{R}_4$	$\omega_4 - \omega_5$	$c = 0$	$\frac{\pi}{4}$

Table 13. Moduli fixing due to $\mathcal{R}J = -J$ and calibration for different choices of the anti-holomorphic involution on the $A_3 \times A_1 \times B_2$ lattice.

which gives rise to the Kähler-form

$$J = 2R_3^2(1+a)\omega_1 + 2R_2^2\omega_2 - 4R_3^2 au_2\omega_3 - R_3R_2(b+2c)\omega_4 - R_3R_2b\omega_5 \qquad (3.34)$$

with the following $\mathbb{Z}_4$-invariant two-forms:

$$
\begin{aligned}
\omega_1 &:= dx^{12} + dx^{23}, \\
\omega_2 &:= dx^{56}, \\
\omega_3 &:= dx^{14} - dx^{24} + dx^{34}, \\
\omega_4 &:= 2dx^{15} - dx^{16} + dx^{26} - 2dx^{35} + dx^{36}, \\
\omega_5 &:= -dx^{16} + 2dx^{25} - dx^{26} + dx^{36}.
\end{aligned}
\qquad (3.35)
$$

The anti-symmetry of the orientifold projection on J leads here again to the fixing of some moduli, as shown in the table 13.

As in the $A_3 \times A_3$-case, we verify that any toroidal $\mathbb{Z}_2$-invariant three-cycle (2.34) is automatically Lagrangian for the choice of fixing the moduli to $b = c = 0$.

Using the complex coordinates (3.13), we can write Ω_3 in real coordinates

$$
\begin{aligned}
\mathrm{Re}(\Omega_3) &= \frac{1}{4\sqrt{u_2}}(\rho_1 + u_1\rho_3 - u_2\rho_4), \\
\mathrm{Im}(\Omega_3) &= \frac{1}{4\sqrt{u_2}}(\rho_2 + u_2\rho_3 + u_1\rho_4),
\end{aligned}
\qquad (3.36)
$$

where the $\mathbb{Z}_4$-invariant three-forms are:

$$
\begin{aligned}
\rho_1 &:= -dx^{125} + dx^{126} - dx^{136} + 2dx^{135} - dx^{235}, \\
\rho_2 &:= -dx^{125} + dx^{136} + dx^{235} - dx^{236}, \\
\rho_3 &:= 2dx^{145} - dx^{146} - dx^{246} - 2dx^{345} + dx^{346}, \\
\rho_4 &:= dx^{146} + 2dx^{245} - dx^{246} - dx^{346}.
\end{aligned}
\qquad (3.37)
$$

The next step is to find the *sLag*s on the orientifolds $T^6/(\mathbb{Z}_4 \times \Omega\mathcal{R}_i)$ with $A_3 \times A_1 \times B_2$ lattice. The *sLag* condition for any three-cycle (2.26) inherited from the torus can be

expressed as follows,

$$\mathrm{Im}(\Omega_3)\,|_{\pi^{\text{torus}}} = \frac{1}{4\sqrt{u_2}}\big([Q-P] + u_1[\bar{P}-\bar{Q}] - u_2[\bar{P}+\bar{Q}]\big)\,, \tag{3.38a}$$

$$\mathrm{Re}(\Omega_3)\,|_{\pi^{\text{torus}}} = \frac{1}{4\sqrt{u_2}}\big([P+Q] - u_1[\bar{P}+\bar{Q}] - u_2[\bar{P}-\bar{Q}]\big)\,, \tag{3.38b}$$

where P, Q, $\bar{P}$, $\bar{Q}$ are the bulk wrapping numbers defined in (2.28). Using this decomposition of a (fraction of a) bulk three-cycle into real and imaginary part in dependence of the complex structure u and the bulk wrapping numbers for the corresponding O6-planes we can calculate the supersymmetry parameters φ_{O6_i} per lattice orientation displayed in table 13.

3.3 Pairwise relations between choices of orientifold axes

We know that in the factorisable case *a priori* six choices of the anti-holomorphic involution are possible, but that there are pairwise relations between them so that only four are physically inequivalent. This means that different but equivalent orientifold projections give rise to the same global semi-realistic particle models as discussed in section 3.1.1.

The same observation can be made in the non-factorisable cases. In order to find these relations between the lattices, we compute all supersymmetric three-cycles which do not overshoot the bulk RR tadpole cancellation condition in (3.1). Together with the supersymmetry conditions (3.24) this gives rise to the restriction on the toroidal and corresponding bulk wrapping numbers, e.g. for the $\mathbf{A_a AB}$-lattice of the $A_3 \times A_1 \times B_2$ lattice, they are bounded by

$$\begin{aligned} A_1 n^3 - A_2 n^3 + 2A_2 m^3 &\leqslant 8\,, \\ 2B_3 n^3 - 2B_2 m^3 &\leqslant 16\,, \end{aligned} \quad \Longleftrightarrow \quad \begin{aligned} P + Q &\leqslant 8\,, \\ \bar{Q} - \bar{P} &\leqslant 16\,. \end{aligned} \tag{3.39}$$

The restrictions on the other lattice orientations take a similar form. The required O6-plane bulk wrapping numbers entering (3.1) are given in (3.12) for the $A_3 \times A_3$ lattice, and in (3.23) for the $A_3 \times A_1 \times B_2$ lattice.

$\mathbf{A_3 \times A_3}$. For this orbifold we found *a priori* four possible involutions. However, due to the relation $\mathcal{R}_4 Q^3 = -\mathcal{R}_1$ between the involutions $\mathcal{R}_1$ and $\mathcal{R}_4$ the $\mathbf{AAA}$- and $\mathbf{BAB}$-lattices give physically identical models on the $A_3 \times A_3$-orientifold. But the relation between the corresponding complex structure values cannot be verified more precisely at this point. There are two possibilities

$$\begin{aligned} &\mathbf{AAA} \text{ dual to } \mathbf{BAB} \text{ and } u_2 = u_2'\,, \\ \text{or} \quad &\mathbf{AAA} \text{ dual to } \mathbf{BAB} \text{ and } u_2 = \frac{1}{u_2'}\,. \end{aligned} \tag{3.40}$$

Moreover, the orientifold projections $\mathcal{R}_2$ and $\mathcal{R}_3$ — corresponding to the $\mathbf{BAA}$ and $\mathbf{AAB}$ lattice orientation, respectively, according to table 12 — act on the three-cycles in the same way, and therefore the supersymmetric three-cycles on the corresponding orientifolds are the same. At first sight one might be tempted to identify these orientifolds, but the

$A_3 \times A_1 \times B_2$-orientifolds			
Lattice	Orien. proj.	# of frac. cycles	# of u_2
$\mathbf{A_a AA}$	$\mathcal{R}_2 \ (u_1 = 0)$	2126	96
$\mathbf{A_a AB}$	$\mathcal{R}_1 \ (u_1 = 0)$	2126	96
$\mathbf{A_a BA}$	$\mathcal{R}_3 \ (u_1 = 0)$	5134	210
$\mathbf{A_a BB}$	$\mathcal{R}_4 \ (u_1 = 0)$	5134	210
$\mathbf{A_b AA}$	$\mathcal{R}_2 \ (u_1 = \frac{1}{2})$	2410	118
$\mathbf{A_b AB}$	$\mathcal{R}_1 \ (u_1 = \frac{1}{2})$	3646	140
$\mathbf{A_b BA}$	$\mathcal{R}_3 \ (u_1 = \frac{1}{2})$	3646	140
$\mathbf{A_b BB}$	$\mathcal{R}_4 \ (u_1 = \frac{1}{2})$	2410	118

Table 14. The number of supersymmetric fractional cycles bounded by the bulk RR tadpole cancellation condition and the number of possible complex structure values u_2 for different choices of orientifold axes.

distinction of the length of the O6-planes, $\pi_{O6_2} = 2\pi_{O6_3}$, gives in principle rise to different allowed ranks and lengths of bulk cycles in the RR tadpole cancellation conditions and consequently to more possible models for the **BAA**-orientifold.

In conclusion, by investigating the structure of bulk three-cycles and their RR tadpole cancellation conditions, we arrive at three physically inequivalent $A_3 \times A_3$-lattice orientations **AAA**, **BAA** and **AAB**.

$\boldsymbol{A_3 \times A_1 \times B_2}$. In this case there are *a priori* eight possible lattice orientations. The number of the corresponding fractional cycles not overshooting the bulk RR tadpole cancellation conditions and the number of possible complex structure values u_2 are presented in the table 14.

Furthermore, we can easily verify the following pairwise relations between the different lattice orientations:

$$
\begin{aligned}
\mathbf{A_a AA} \text{ dual to } \mathbf{A_a AB} \text{ and } u_2 &= \frac{1}{2u_2'} \,, \\
\mathbf{A_a BA} \text{ dual to } \mathbf{A_a BB} \text{ and } u_2 &= \frac{1}{2u_2'} \,, \\
\mathbf{A_b AA} \text{ dual to } \mathbf{A_b BB} \text{ and } u_2 &= \frac{1}{4u_2'} \,, \\
\mathbf{A_b BA} \text{ dual to } \mathbf{A_b AB} \text{ and } u_2 &= \frac{1}{4u_2'} \,.
\end{aligned}
\tag{3.41}
$$

Altogether, we have thus four physically inequivalent lattices (two with $u_1 = 0$ and two with $u_1 = \frac{1}{2}$) and can restrict our further considerations to the lattice orientations **AAB** and **ABB**.

3.4 Cross-check: D6-branes on top of O6-planes

Non-factorisable $T^6/\mathbb{Z}_4$ orbifolds have been briefly studied in the past. For instance, in [63] only D6-branes on top of the orientifold planes were considered, and only for a particular choice of the moduli in (2.13) and (2.25), i.e., the radii of all tori being equal and all the tori being orthogonal to each other. Our goal in this section is twofold. At first, we will reproduce and extend the CFT methods and results of [63] to arbitrary values of the moduli, in particular providing the Kaluza-Klein and winding modes for generic D6-brane configuration. Secondly, we will compare this result with the geometric method described earlier on, i.e. by requiring that the *sLag* three-cycles wrapped by generic D6-branes satisfy the RR tapdole cancellation condition (3.1) — in the case at hand with only two stacks of D6-branes.

Let us start by reviewing the method used in [63]. We denote a basis of the torus lattice by $\{e_i\}$. Let $\{e_i^*\}$ be a basis of the dual lattice such that $e_i \cdot e_j^* = \delta_{ij}$. If the lattice vectors e_i form the Q-invariant metric g_{ij}, the dual vectors $\{e_i^*\}$ form the metric $g_{ij}^* = e_i^* \cdot e_j^* = g_{ij}^{-1}$. Note that the dual vectors transform under Q^t and $\mathcal{R}_{m\,(m=1,2,3,4)}^t$.

In general, insertions of $\Omega\mathcal{R}_m Q^{2k}$ and $\Omega\mathcal{R}_m Q^{2k+1}$ in the Klein bottle trace (and strings starting on the 6_{2k} and 6_{2k+1} branes in the annulus and Möbius strip) give different lattice contributions, so we need to compute both cases separately. In the rest of this section we will only consider the first case, but the second one is obtained analogously, by replacing $\mathcal{R}_m$ by $\mathcal{R}_m Q$ throughout the elaboration.

Let $\mathbf{v}_i$ ($i = 1, 2, 3$) be the lattice vectors that span the (fraction of the) bulk three-cycle wrapped by the O6-plane. They satisfy $\mathcal{R}_m\mathbf{v}_i = \mathbf{v}_i$. The winding modes are described by vectors $\mathbf{w}_i$, $i = 1, 2, 3$, satisfying $\mathcal{R}_m\mathbf{w}_i = -\mathbf{w}_i$. The momentum modes $\mathbf{p}_i$ appearing in the Klein bottle amplitude in sectors where there are fixed tori correspond to vectors in the dual lattice invariant under $\mathcal{R}_m$. Using all these vectors we define the matrices

$$(M_{KB})_{ij} := \mathbf{p}_i \cdot \mathbf{p}_j \,, \tag{3.42}$$

$$(M_A)_{ij} = (M_{MS})_{ij} := \mathbf{v}_i \cdot \mathbf{v}_j \,, \tag{3.43}$$

$$(W_{KB})_{ij} = (W_{MS})_{ij} := \mathbf{w}_i \cdot \mathbf{w}_j \,. \tag{3.44}$$

The lattice mode contributions (in the corresponding sector) for the Klein bottle, annulus, and Möbius strip are

$$KB = \frac{4^n}{(\det M_{KB} \det W_{KB})^{1/2}} \,, \tag{3.45}$$

$$A = \frac{\det M_A}{(\det g)^{1/2}} \,, \tag{3.46}$$

$$MS = \frac{4^n(\det M_{MS})^{1/2}}{(\det W_{MS})^{1/2}} \,, \tag{3.47}$$

where $n = \dim(M) = \dim(W)$, ($n = 3$ in the untwisted sector, which is the one we are interested in).

The tadpole cancellation condition is then given by

$$KB + \frac{M^2 \cdot A}{16} - \frac{M \cdot MS}{16} = 0 \tag{3.48}$$

where M is the number of identical branes (in the $\mathcal{R}_m Q$ case we will denote it by N).

$\mathbf{A_3 \times A_3}$. Let us start with the $A_3 \times A_3$ lattice. For concreteness, we will focus on the orientation **AAB**. We will show that the number of supersymmetric D6-branes needed to cancel the (bulk) RR tadpole depends on the angle-moduli between the two A_3-tori.

Recall that for the orientifold **AAB** we have the involution $\mathcal{R}_3$ (3.7), which fixes the moduli to $c + e = 0$ (as consequence of $u_1 = 0$) and $e + d = 0$ (see table 12). Using these constraints and the Q-invariant metric g, we obtain the following momentum modes $\mathbf{p}_i$:

$$\mathbf{p}_1 = 2e_1^* - e_2^*, \tag{3.49}$$

$$\mathbf{p}_2 = e_1^* - e_3^*, \tag{3.50}$$

$$\mathbf{p}_3 = e_4^* + e_5^* - e_6^*. \tag{3.51}$$

The winding modes are:

$$\mathbf{w}_1 = e_1 + 2e_2 + e_3, \tag{3.52}$$

$$\mathbf{w}_2 = e_4 - e_5, \tag{3.53}$$

$$\mathbf{w}_3 = e_4 + e_6. \tag{3.54}$$

The $\mathbf{v}_i$ vectors spanning the O6-planes are:

$$\mathbf{v}_1 = e_1, \tag{3.55}$$

$$\mathbf{v}_2 = e_3, \tag{3.56}$$

$$\mathbf{v}_3 = e_4 + e_5. \tag{3.57}$$

The determinants of the corresponding matrices M_{KB}, M_A and W_{KB} are

$$\begin{aligned} \det M_{KB} &= -\frac{2}{a(1 + a + b + ab - 2e^2)R_1^4 R_2^2}, \\ \det M_A &= -8a(1 + a + b + ab - 2e^2)R_1^4 R_2^2, \\ \det W_{KB} &= -32b(1 + a + b + ab - 2e^2)R_1^2 R_2^4. \end{aligned} \tag{3.58}$$

They give rise to the lattice mode contributions to the untwisted sector

$$KB = 8\sqrt{\frac{a}{b}}\frac{R_1}{R_2}, \qquad A = 2\sqrt{\frac{a}{b}}\frac{R_1}{R_2}, \qquad MS = 32\sqrt{\frac{a}{b}}\frac{R_1}{R_2}. \tag{3.59}$$

The untwisted RR tadpole cancellation condition is

$$KB + \frac{M^2 \cdot A}{16} - \frac{M \cdot MS}{16} = 0 \Rightarrow (M - 8)^2 = 0. \tag{3.60}$$

The $\mathcal{R}_3 Q$-case leads to the analogous result $(N - 8)^2 = 0$. Due to the action of the $\mathbb{Z}_2$ symmetry on the corresponding Chan-Paton factors, the gauge group will have rank $\frac{M}{2} \times \frac{N}{2}$,

$A_3 \times A_3$ orientifolds with D-branes on top of the O-plane				
$A_3 \times A_3$		General	$e = 0$	
Lattice	Involution	$M = N$	$M = N$	Gauge group
AAA	$\mathcal{R}_1$	8	8	$\mathrm{USp/SO}(8) \times \mathrm{USp/SO}(8)$
BAA	$\mathcal{R}_2$	8	8	$\mathrm{USp/SO}(8) \times \mathrm{USp/SO}(8)$
AAB	$\mathcal{R}_3$	8	8	$\mathrm{USp/SO}(8) \times \mathrm{USp/SO}(8)$
BAB	$\mathcal{R}_4$	8	8	$\mathrm{USp/SO}(8) \times \mathrm{USp/SO}(8)$

Table 15. IIA Orientifolds of $\mathbb{Z}_4$-orbifolds with the lattice of the type $A_3 \times A_3$ with D-branes on O-plane. For generic values of the metric moduli, the gauge group is $\mathrm{U}\left(\frac{M}{2}\right) \times \mathrm{U}\left(\frac{N}{2}\right)$.

and the gauge group for generic values of moduli is $\mathrm{U}(4) \times \mathrm{U}(4)$ (with a possible gauge symmetry enhancement $\mathrm{U}(4) \hookrightarrow \mathrm{USp/SO}(8)$,[6] for special choices of geometric moduli — in particular for the choice $c = d = e = 0$ of the two A_3 lattices orthogonal to each other in (2.13) —, where determining the appropriate type of symmetry enhancement requires the development of CFT techniques at one-loop so far only available for $(T^2)^3$ factorisable backgrounds, see e.g. [37, 73, 79, 80, 96]).

The complementary purely geometric considerations are as follows: the cycle wrapped by the O6-plane is $-2\gamma_1 - 2\bar{\gamma}_2$. For $e = 0$, its contribution to the tadpole can be cancelled by a stack of $N_1 = 4$ branes wrapping the cycle $-\gamma_1$ and a second stack of $N_2 = 4$ branes wrapping $-\bar{\gamma}_2$, giving rise to a gauge group $\mathrm{USp/SO}(8) \times \mathrm{USp/SO}(8)$ in agreement with the CFT result.

The results for the remaining orientifold projections are summarised in the table 15.

$A_3 \times A_1 \times B_2$. Let us now consider the $A_3 \times A_1 \times B_2$ lattice. For simplicity we will present the analysis of the case where the B_2-torus is orthogonal to $A_3 \times A_1$. This means that the moduli b, c vanish.[7] For the explicit computations, we will focus on the $\mathcal{R}_1$ involution (3.15).

A_aAB. The condition $u_1 = 0$ restricts the moduli d and a. From the definition of the complex structure modulus (3.14) we obtain that d is fixed to 0 and a has to be negative.

Since the dual basis vectors e_i^* transform under the transposed orientifold action $\mathcal{R}_1^t$, the momentum modes $\mathbf{p}_i$ are the eigenvectors of $\mathcal{R}_1^t$ to the eigenvalue $+1$:

$$\begin{aligned}
\mathbf{p}_1 &= e_1^* - e_3^*, \\
\mathbf{p}_2 &= 2e_1^* - e_2^* + e_3^*, \\
\mathbf{p}_3 &= e_5^* + e_6^*.
\end{aligned} \qquad (3.61)$$

---

[6]This is a shorthand notation for either $\mathrm{USp}(8)$ or $\mathrm{SO}(8)$.

[7]For an arbitrary choice of these moduli (up to the moduli fixing in table 13), we obtain the same results.

The winding modes are

$$\begin{aligned}
\mathbf{w}_1 &= e_1 + 2e_2 + e_3\,, \\
\mathbf{w}_2 &= e_4\,, \\
\mathbf{w}_3 &= e_5 - e_6\,,
\end{aligned} \tag{3.62}$$

and the $\mathbf{v}_i$ vectors describing the bulk part of a fractional cycle parallel to some O6-plane are

$$\begin{aligned}
\mathbf{v}_1 &= e_1\,, \\
\mathbf{v}_2 &= e_3\,, \\
\mathbf{v}_3 &= e_5 + e_6\,.
\end{aligned} \tag{3.63}$$

The determinants of the different matrices are

$$\det M_{KB} := -\frac{2}{a(1+a)R_3^4 R_2^2}\,, \quad \det M_A := -8a(1+a)R_3^4 R_2^2\,, \quad \det W_{KB} := 8(1+a)R_3^2 R_2^2 R_1^2\,. \tag{3.64}$$

The lattice mode contributions to the untwisted sector are

$$KB = 16\sqrt{-a}\frac{R_3}{R_1}\,, \qquad A = 4\sqrt{-a}\frac{R_3}{R_1}\,, \qquad MS = 64\sqrt{-a}\frac{R_3}{R_1}\,, \tag{3.65}$$

and the corresponding untwisted RR tadpole cancellation condition reads

$$KB + \frac{M^2 \cdot A}{16} - \frac{M \cdot MS}{16} = 0 \Rightarrow (M - 8)^2 = 0\,. \tag{3.66}$$

Thus, we get $M = 8$ which agrees with [63]. In a similar way one shows that the tadpole condition from the $\mathcal{R}_1 Q$-part gives rise to $N = 16$. The resulting gauge group is thus $\mathrm{U}(4) \times \mathrm{U}(8)$ or some rank preserving gauge enhancement to $\mathrm{SO}(2M)$ or $\mathrm{USp}(2M)$ (for one or both gauge factors).

The CFT calculation is complemented by purely geometric considerations as follows: the cycle wrapped by the O6-planes is $\gamma_1 + \gamma_2 - 2(\bar\gamma_1 - \bar\gamma_2)$. Its contribution to the tadpole can be cancelled by a stack of $N_1 = 4$ branes wrapping the fractional cycle $\frac{1}{2}\gamma_1 + \frac{1}{2}\gamma_2$ and a stack of $N_2 = 8$ branes wrapping $-\frac{1}{2}\bar\gamma_1 + \frac{1}{2}\bar\gamma_2 \pm \frac{1}{2}\bar\gamma_3 \pm \frac{1}{2}\bar\gamma_4$ (any choice of sign for the exceptional part is allowed). Since the first stack is invariant under the orientifold action, the actual gauge group is $\mathrm{SO}/\mathrm{USp}(8) \times \mathrm{U}(8)$. Our result — which agrees for both (CFT and cycle homology) methods — differs slightly from [63] in the fact that the first gauge factor experiences a gauge group enhancement, which they do not mention.

$\mathbf{A_b AB}$. In this case, from the condition $u_1 = \frac{1}{2}$ we obtain

$$d = -\frac{aR_3}{R_1}\,, \qquad a\left(1 + a\frac{R_3^2}{R_1^2}\right) < 0\,. \tag{3.67}$$

The momentum modes $\mathbf{p}_i$ are

$$\begin{aligned}
\mathbf{p}_1 &= e_1^* - e_3^*\,, \\
\mathbf{p}_2 &= 2e_1^* - e_2^* + e_4^*\,, \\
\mathbf{p}_3 &= e_6^*\,.
\end{aligned} \tag{3.68}$$

$A_3 \times A_1 \times B_2$ orientifolds with D-branes on top of the O-planes							
$A_3 \times A_1 \times B_2$		$u_1 = 0$			$u_1 = \frac{1}{2}$		
Lattice	Involution	M	N	Gauge group	M	N	Gauge group
AAA	$\mathcal{R}_2$	16	8	U(8) × USp/SO(8)	16	4	U(8) × USp/SO(4)
AAB	$\mathcal{R}_1$	8	16	USp/SO(8) × U(8)	8	8	USp/SO(8) × U(4)
ABA	$\mathcal{R}_3$	16	8	U(8) × USp/SO(8)	8	8	U(8) × USp/SO(8)
ABB	$\mathcal{R}_4$	8	16	USp/SO(8) × U(8)	4	16	USp/SO(4) × U(8)

Table 16. IIA Orientifolds of $\mathbb{Z}_4$-orbifolds with the lattice of the type $A_3 \times A_1 \times B_2$ with D-branes on top of the O-planes canceling the RR tadpoles.

The winding modes $\mathbf{w}_i$ and lattice vectors $\mathbf{v}_i$ are

$$\mathbf{w}_1 = e_1 + 2e_2 + e_3 \,,$$
$$\mathbf{w}_2 = e_2 + e_4 \,,$$
$$\mathbf{w}_3 = e_5 \,, \tag{3.69}$$
$$\mathbf{v}_1 = e_1 \,,$$
$$\mathbf{v}_2 = e_3 \,, \tag{3.70}$$
$$\mathbf{v}_3 = e_5 + 2e_6 \,.$$

The determinants of the different matrices are thus given by

$$\det M_{KB} = \frac{-2}{(a+a^2)R_2^2 R_3^4} \,, \quad \det M_A = -8(1+a)aR_2^2 R_3^4 \,, \quad \det W_{KB} = 8(1+a)(R_1^2 + aR_3^2)R_2^2 R_3^2 \,, \tag{3.71}$$

and the resulting untwisted RR tadpole cancellation condition reads

$$KB + \frac{M^2 \cdot A}{16} - \frac{M \cdot MS}{16} = 0 \Rightarrow (M - 8)^2 = 0 \,, \tag{3.72}$$

i.e. we obtain $M = 8$. In a similar manner, the $\mathcal{R}_1 Q$-insertion gives rise to $N = 8$. Therefore, the gauge group is U(4)×U(4) or some rank preserving gauge group enhancement thereof.

The complementary considerations in terms of cycle homologies are as follows: the cycle wrapped by the O6-planes is $2\gamma_2 - 2(\bar{\gamma}_1 - \bar{\gamma}_2)$. Its contribution to the tadpole can be cancelled, for instance, by a stack of $N_1 = 4$ branes wrapping the fractional cycle $\frac{1}{2}\gamma_1 + \frac{1}{2}\gamma_2$ and a stack of $N_2 = 4$ branes wrapping $-\frac{1}{2}\gamma_1 + \frac{1}{2}\gamma_2 - \bar{\gamma}_1 + \bar{\gamma}_2 \pm \left(\frac{1}{2}\gamma_3 - \bar{\gamma}_3\right) \pm \left(\frac{1}{2}\gamma_4 - \bar{\gamma}_4\right)$ (any choice of sign for the exceptional part is allowed). Naively, this gives rise to the gauge group U(4) × U(4), but the first stack maps to itself under the orientifold action, which enhances the symmetry to USp/SO(8) × U(4).

The results for the remaining orientifold projections can be derived analogously and are summarised in the table 16.

The column $u_1 = 0$ agrees mostly with the result [63], while the results for $u_1 = \frac{1}{2}$ are presented here for the first time. We can also see the relation between the lattices (3.41) if we interchange M and N.

4 Factorisation of non-factorisable orbifolds

In this section we will show that both non-factorisable orbifolds can be written in a factorised form. This identification between the lattices was already detected in [97] by consideration of factorisable orbifolds. Here we want to explain which conclusions this identification means from the point of view of non-factorisable orbifolds. We make the restriction that in the first non-factorisable orbifold background, both A_3 lattices are orthogonal to each other, and in the second non-factorisable orbifold background, the $A_3 \times A_1$ lattice is orthogonal to the B_2 lattice. This fixes the moduli to $c = d = e = 0$ and $b = c = 0$, respectively. On both orbifolds we can find a real basis such that the non-factorisable structure of the lattice decomposes into three two-tori, but an additional $\mathbb{Z}_2$ shift symmetry appears. Any three-cycle, written now as a product of three one-cycles on each two-torus, is automatically $\mathbb{Z}_2$-invariant. Moreover, only $\mathbb{Z}_2$-invariant three-cycles on the non-factorisable lattice can be expressed as three-cycles with respect to the new basis. Therefore, the number of wrapping numbers is reduced from twelve ($A_3 \times A_3$) or ten ($A_3 \times A_1 \times B_2$) to six in agreement with the naive expectation from the known factorisable orbifold backgrounds $(T^2)^3/\mathbb{Z}_N$ or $(T^2)^3/(\mathbb{Z}_N \times \mathbb{Z}_M)$.[8]

Because any three-cycle, written in the new basis, is $\mathbb{Z}_2$-invariant, it follows that it is automatically Lagrangian. Furthermore, it can be verified that the *sLag* condition can be expressed in the same form as for the usual factorisable orbifolds: the sum of the angles between the one-cycles wrapped by supersymmetric D6-branes on each two-torus and the $\mathcal{R}_i$-invariant O6-plane has to vanish (mod 2π).

$A_3 \times A_3$. In this case, we introduce new coordinates along the directions

$$
\begin{aligned}
v_1 &:= \pi_1 + \pi_2, & v_2 &:= \pi_2 + \pi_3, & v_3 &:= \pi_1 + \pi_3, \\
v_4 &:= \pi_4 + \pi_6, & v_5 &:= \pi_4 + \pi_5, & v_6 &:= \pi_5 + \pi_6.
\end{aligned}
\tag{4.1}
$$

With respect to this basis, the metric g and the Coxeter element Q take a factorised form,

$$
g = \text{diag}\left(2(1+a)R_1^2,\ 2(1+a)R_1^2,\ -4aR_1^2,\ -4bR_2^2,\ 2(1+b)R_2^2,\ 2(1+b)R_2^2\right),
\tag{4.2}
$$

$$
Q = \text{diag}\begin{pmatrix} 0 & -1 \\ 1 & 0 \end{pmatrix} \oplus \begin{pmatrix} -1 & 0 \\ 0 & -1 \end{pmatrix} \oplus \begin{pmatrix} 0 & -1 \\ 1 & 0 \end{pmatrix},
\tag{4.3}
$$

and also the orientifold projections $\mathcal{R}_i$ become factorised, e.g.:

$$
\mathcal{R}_4 = \text{diag}\begin{pmatrix} 1 & 0 \\ 0 & -1 \end{pmatrix} \oplus \begin{pmatrix} 1 & 0 \\ 0 & -1 \end{pmatrix} \oplus \begin{pmatrix} 1 & 0 \\ 0 & -1 \end{pmatrix}.
\tag{4.4}
$$

---

[8]Note, however, that due to the additional symmetry some of the new wrapping numbers can now also be half-integer.
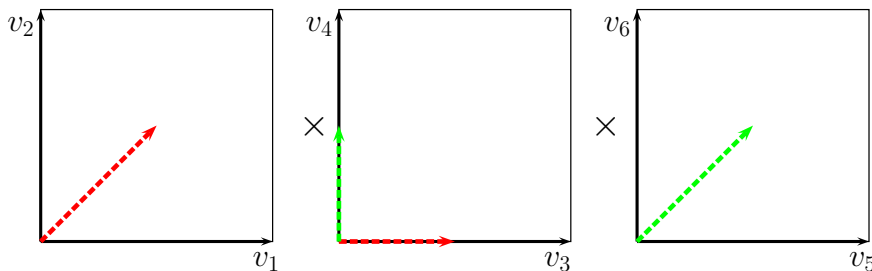
Figure 9. Shift identifications of points on the factorised form of the $A_3 \times A_3$-lattice by $\frac{v_1 + v_2 + v_3}{2}$ (red) and $\frac{v_4 + v_5 + v_6}{2}$ (green).

But as already mentioned, the basis change gives rise to additional symmetries, which identify points of the factorised torus by the following shifts

$$
\begin{aligned}
p &\simeq p + \frac{v_1 + v_2 + v_3}{2}\,, \\
p &\simeq p + \frac{v_4 + v_5 + v_6}{2}\,,
\end{aligned}
\tag{4.5}
$$

for any point p on the torus, as depicted in figure 9.

In the new coordinates, only six wrapping numbers occur,

$$
\pi^{\text{torus}} := (\tilde{n}^1 v_1 + \tilde{m}^1 v_2) \wedge (\tilde{n}^2 v_3 + \tilde{m}^2 v_4) \wedge (\tilde{n}^3 \pi_5 + \tilde{m}^3 \pi_6)\,,
\tag{4.6}
$$

in terms of which the bulk wrapping numbers defined in (2.14) and (2.16) can be rewritten as follows:

$$
\begin{aligned}
A_1 q^1 &= -A_3 q^1 = -(\tilde{n}^1 + \tilde{m}^1)\tilde{n}^2 \tilde{n}^3, & B_1 m^1 &= -B_3 m^1 = \tilde{n}^1 \tilde{m}^2 (\tilde{n}^3 + \tilde{m}^3)\,, \\
A_1 r^1 &= -A_3 r^1 = -(\tilde{n}^1 + \tilde{m}^1)\tilde{n}^2 (\tilde{n}^3 + \tilde{m}^3)\,, & B_1 n^1 &= -B_3 n^1 = (\tilde{n}^1 + \tilde{m}^1)\tilde{m}^2 (\tilde{n}^3 + \tilde{m}^3)\,, \\
A_1 s^1 &= -A_3 s^1 = -(\tilde{n}^1 + \tilde{m}^1)\tilde{n}^2 \tilde{m}^3, & B_1 p^1 &= -B_3 p^1 = \tilde{m}^1 \tilde{m}^2 (\tilde{n}^3 + \tilde{m}^3)\,, \\
A_2 q^1 &= (\tilde{n}^1 - \tilde{m}^1)\tilde{n}^2 \tilde{n}^3, & B_2 m^1 &= \tilde{n}^1 \tilde{m}^2 (-\tilde{n}^3 + \tilde{m}^3)\,, \\
A_2 r^1 &= (\tilde{n}^1 - \tilde{m}^1)\tilde{n}^2 (\tilde{n}^3 + \tilde{m}^3)\,, & B_2 n^1 &= (\tilde{n}^1 + \tilde{m}^1)\tilde{m}^2 (-\tilde{n}^3 + \tilde{m}^3)\,, \\
A_2 s^1 &= (\tilde{n}^1 - \tilde{m}^1)\tilde{n}^2 \tilde{m}^3, & B_2 p^1 &= \tilde{m}^1 \tilde{m}^2 (-\tilde{n}^3 + \tilde{m}^3)\,.
\end{aligned}
\tag{4.7}
$$

Note that due to the shift symmetry (4.5), the wrapping numbers $\tilde{n}^2$ and $\tilde{m}^2$ can also have half-integer values.

On the factorised lattice, the geometric difference between the length of the O6-planes on the **AAB**- and **BAA**-orientations becomes clear: for the **AAB**-lattice, the $\mathcal{R}$-invariant O6-plane is placed along the axes $v_1 - v_2$ and v_3 on $T^2_{(1)} \times T^2_{(2)}$ and therefore it passes through the points which are identified by the shift symmetry (4.5), but this is no longer the case for the **BAA**-lattice.

$\boldsymbol{A_3 \times A_1 \times B_2}$. Here it suffices to introduce new directions only on $A_3 \times A_1$:

$$
\begin{aligned}
v_1 &:= \pi_1 + \pi_2\,, & v_3 &:= \pi_1 + \pi_3\,, \\
v_2 &:= \pi_2 + \pi_3\,, & v_4 &:= \pi_4\,.
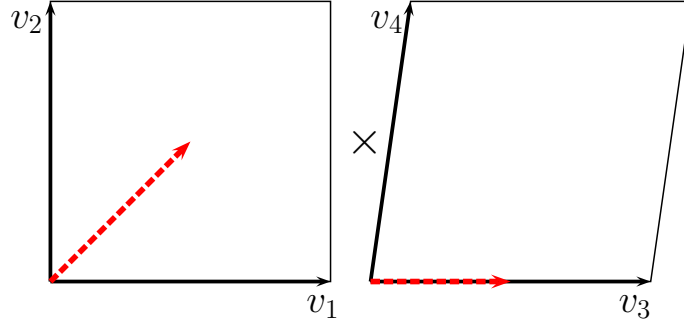\end{aligned}
\tag{4.8}
$$

Figure 10. Shift symmetry of the factorised form of the $A_3 \times A_1$-lattice along $\frac{v_1+v_2+v_3}{2}$ (in red).

This basis factorises the torus, such that the metric becomes

$$g = \text{diag} \begin{pmatrix} 2(1+a)R_3^2 & 0 \\ 0 & 2(1+a)R_3^2 \end{pmatrix} \oplus \begin{pmatrix} -4aR_3^2 & -4au_1R_3^2 \\ -4au_1R_3^2 & R_1^2 \end{pmatrix} \oplus \begin{pmatrix} 2R_2^2 & -R_2^2 \\ -R_2^2 & R_2^2 \end{pmatrix}. \quad (4.9)$$

For the Coxeter element Q and the orientifold projections $\mathcal{R}_i$ we obtain

$$Q = \text{diag} \begin{pmatrix} 0 & -1 \\ 1 & 0 \end{pmatrix} \oplus \begin{pmatrix} -1 & 0 \\ 0 & -1 \end{pmatrix} \oplus \begin{pmatrix} 1 & -1 \\ 2 & -1 \end{pmatrix}, \quad (4.10)$$

$$\mathcal{R}_1 = \text{diag} \begin{pmatrix} 0 & -1 \\ -1 & 0 \end{pmatrix} \oplus \begin{pmatrix} 1 & 2u_1 \\ 0 & -1 \end{pmatrix} \oplus \begin{pmatrix} 1 & -1 \\ 0 & -1 \end{pmatrix}, \quad (4.11)$$

$$\mathcal{R}_4 = \text{diag} \begin{pmatrix} -1 & 0 \\ 0 & 1 \end{pmatrix} \oplus \begin{pmatrix} 1 & 2u_1 \\ 0 & -1 \end{pmatrix} \oplus \begin{pmatrix} 1 & -1 \\ 0 & -1 \end{pmatrix}. \quad (4.12)$$

Also in this case the basis change gives rise to an additional shift symmetry displayed in figure 10,

$$p \simeq p + \frac{v_1 + v_2 + v_3}{2} \quad \text{for any point } p \text{ on the torus}. \quad (4.13)$$

Instead of ten wrapping numbers which we need to describe a fractional three-cycle in non-factorisable coordinates, in the v-basis the usual six wrapping numbers are sufficient:

$$\pi^{\text{torus}} := (\tilde{n}^1 v_1 + \tilde{m}^1 v_2) \wedge (\tilde{n}^2 v_3 + \tilde{m}^2 v_4) \wedge (m^3 \pi_5 + n^3 \pi_6). \quad (4.14)$$

The relation between the non-factorised toroidal and bulk wrapping numbers in (2.26) and (2.29) and the new factorised ones is given by

$$\begin{aligned} A_1 &= -A_3 = -(\tilde{n}^1 + \tilde{m}^1)\tilde{n}^2, & A_2 &= (\tilde{n}^1 - \tilde{m}^1)\tilde{n}^2, \\ B_1 &= \tilde{n}^1 \tilde{m}^2, & B_3 &= \tilde{m}^1 \tilde{m}^2 = B_2 - B_1. \end{aligned} \quad (4.15)$$

Notice that here, due to the shift symmetry (4.13), the wrapping number $\tilde{n}^2$ can be half-integer if $\tilde{m}^1 + \tilde{n}^1$ is even.

$A_3 \times A_1 \times B_2$		
	Two generations	Four generations
$\mathbf{A_a AB}$	$\infty, 1$	$\infty, 1$
$\mathbf{A_b AB}$	∞	∞
$\mathbf{A_a BB}$	$\infty, 1, 3, \frac{1}{2}, \frac{1}{3}, \frac{1}{4}, \frac{1}{6}, \frac{1}{8}, \frac{1}{9}, \frac{1}{12}$	$\infty, 1, 2, \frac{1}{2}, \frac{1}{3}, \frac{1}{4}, \frac{1}{6}, \frac{1}{9}, \frac{1}{12}$
$\mathbf{A_b BB}$	$\infty, 1, \frac{1}{4}$	$-$

Table 17. The possible values of $\mathrm{Im}(\mathcal{U})$ for global supersymmetric Pati-Salam models, with ∞ denoting that it can be choosen arbitrarily.

5 Concrete Pati-Salam models on $A_3 \times A_1 \times B_2$

In this section we present the construction of some local and global semi-realistic supersymmetric Pati-Salam (PS) models using intersecting D6-branes.[9] In section 3.3 we have seen that there exist duality relations between the different orientifold projections $\mathcal{R}_i$ ($i = 1, 2, 3, 4$) and that only four lattice orientations are independent. For the construction of particle spectra, we choose the **AAB**- and **ABB**-types lattices. In addition to the RR tadpole cancellation and $sLag$ conditions, we require that the $\mathrm{U}(4)_a$ stack is free from (anti-)symmetric representations.[10] An intensive computer search showed that only global supersymmetric PS-models with two or four generations are possible. The supersymmetry conditions give rise to restrictions on the allowed values of the imaginary part u_2 of the complex structure modulus $\mathcal{U}$, and only a small number of values can be used for the construction of global PS-models without overshooting the bulk RR tadpole cancellation condition. The allowed values of u_2 are illustrated in the table 17. For some branes, some bulk wrapping numbers turn out to be zero, and thus the supersymmetry conditions do not fix the complex structure. If PS-models can be constructed just with such branes, we will list the arbitrariness in $\mathrm{Im}(\mathcal{U})$ as ∞ in table 17.

Two generations. We start the search for global PS-models with the case of two particle generations and note some general properties of the models obtained. All models with $\mathrm{U}(4) \times \mathrm{U}(2) \times \mathrm{U}(2)$-gauge group in the visible sector contain chiral particles which transform in the (anti-)symmetric representation of the $\mathrm{U}(2)$ on the b and/or c-stack. The spectrum of the models with gauge symmetry enhancement $\mathrm{U}(1) \hookrightarrow \mathrm{USp}/\mathrm{SO}(2)$ on both the b- and c-stack, on the other hand, lacks the bifundamental representations in the bc-sector, i.e., there is no Higgs field in the chiral spectrum of such models. In table 18, we provide an explicit example of a PS-model with $\mathrm{U}(4) \times \mathrm{U}(2) \times \mathrm{USp}/\mathrm{SO}(2)$ gauge group in the visible sector. Its chiral spectrum is given in the table 19.

---

[9]Notice that for generic configurations of gauge groups, *global* models do not only have to satisfy the RR tadpole cancellation conditions, but also the K-theory constraints, which are usually derived by scanning through all possible probe D-branes supporting $\mathrm{USp}(2)$ gauge factors [98]. For PS models with all gauge groups (including 'hidden' ones) of even rank, the K-theory constraints are, however, trivially fulfilled.

[10]The systematic computer search on the $A_3 \times A_1 \times B_2$ lattices actually showed that all two- and four-generation models of PS-type satisfy this condition without *a priori* imposing it.

D6-branes configuration for two generation PS-model on $A_3 \times A_1 \times B_2$-orientifold		
Stack	$(m^1, n^1, p^1, q^1) \times (m^2, n^2, p^2, q^2) \times (m^3, n^3)$	Homology cycle
$\mathrm{U}(4)_a$	$(1, 0, -1, 0) \times (1, 0, 0, 1) \times (-1, -2)$	$\frac{1}{2}\gamma_1 - \frac{1}{2}\gamma_2 - \bar{\gamma}_1 + \bar{\gamma}_2$
$\mathrm{U}(2)_b$	$(0, 1, 1, 0) \times (0, 0, 0, 1) \times (1, 2)$	$\bar{\gamma}_2 - \bar{\gamma}_3 + \bar{\gamma}_4$
$\mathrm{USp/SO}(2)_c$	$(1, 1, 0, 0) \times (1, 0, 1, 0) \times (-1, -2)$	$\gamma_1 + \gamma_3 - \gamma_4$
$\mathrm{USp/SO}(2)_{h_1}$	$(1, 1, 0, 0) \times (1, 0, 1, 0) \times (-1, -2)$	$\gamma_1 - \gamma_3 + \gamma_4$
$\mathrm{U}(2)_{h_2}$	$(0, 1, 1, 0) \times (0, 0, 0, 1) \times (1, 2)$	$\bar{\gamma}_2 - \bar{\gamma}_3 - \bar{\gamma}_4$

Table 18. D6-branes for a two generation supersymmetric PS-model with $\mathbf{A_aBB}$-lattice and $u_2 = 1/2$.

Chiral spectrum of two generation PS-model on $A_3 \times A_1 \times B_2$-orientifold	
Sector	$\mathrm{SU}(4)_a \times \mathrm{SU}(2)_b \times \mathrm{USp/SO}(2)_c \times \mathrm{USp/SO}(2)_{h_1} \times \mathrm{SU}(2)_{h_2} \times \mathrm{U}(1)^3$
ab	$(4, \bar{2}, 1, 1, 1)_{(1,-1,0)}$
ab'	$(4, 2, 1, 1, 1)_{(1,1,0)}$
$ac = ac'$	$2 \times (\bar{4}, 1, 2, 1, 1)_{(-1,0,0)}$
$bc = bc'$	$4 \times (1, 2, \bar{2}, 1, 1)_{(0,1,0)}$
$ah_1 = ah_1'$	$2 \times (\bar{4}, 1, 1, 2, 1)_{(-1,0,0)}$
$bh_1 = bh_1'$	$4 \times (1, 2, 1, \bar{2}, 1)_{(0,-1,0)}$
ah_2	$(4, 1, 1, 1, \bar{2})_{(1,0,-1)}$
ah_2'	$(4, 1, 1, 1, 2)_{(1,0,1)}$

Table 19. Chiral spectrum for the two generation $\mathrm{U}(4) \times \mathrm{U}(2) \times \mathrm{USp/SO}(2) \times \mathrm{USp/SO}(2) \times \mathrm{U}(2)$-PS model with D6-brane configuration given in table 18.

In appendix A, we provide an explicit example for each other type of visible gauge group, i.e. $\mathrm{U}(4) \times \mathrm{U}(2) \times \mathrm{U}(2)$ and $\mathrm{U}(4) \times \mathrm{USp/SO}(2) \times \mathrm{USp/SO}(2)$.

Four generations. In a similar way, we can realise global supersymmetric PS-models with four generations with different gauge groups (without/with some enhancement of the 'left' and 'right' stack) in the visible sector. In general, only the $\mathrm{U}(4) \times \mathrm{USp/SO}(2) \times \mathrm{USp/SO}(2)$-models do not contain chiral matter in the (anti-)symmetric representation on the b- and c- stacks. But these models also do not contain chiral states in the bifundamental representation of the bc-sector, which could serve as a (chiral) Higgs multiplet. In appendix A, we collect several examples of global D6-brane configurations of such types together with their chiral spectrum.

Three generations. As mentioned above, there are no global supersymmetric Pati-Salam models with three generations. But it is possible to construct models where the bulk part of the tadpole vanishes and only the exceptional part remains. Such *local* models are only realisable on the $\mathbf{ABB}$-orientifolds. More precisely, for the $\mathbf{A_aBB}$-lattice only $u_2 = 3, \frac{1}{3}$ provides such models, and the gauge group is enhanced on the b- and c-stacks.

For the $\mathbf{A_b BB}$-lattice, it is possible to construct *local* models with $u_2 = \frac{3}{2}$ with symmetry enhancement on the b- and/or c-stack. A general property of all such models is the appearance of chiral particles which transform in the (anti-)symmetric representation of $U(4)_a$.

6 Discussion and conclusions

In this article, we explored the full three-cycle geometry of the non-factorisable $T^6/\mathbb{Z}_4$ orbifold on the two possible root lattices $A_3 \times A_3$ and $A_3 \times A_1 \times B_2$ and compared it with the factorisable $B_2 \times (A_1)^2 \times B_2$ case. We found that, under the anti-holomorphic involution $\mathcal{R}$ of Type IIA/$\Omega\mathcal{R}$ orientifolds, there exist *a priori* four different lattice orientations for $A_3 \times A_3$, and eight for $A_3 \times A_1 \times B_2$. However, a closer look at the number of supersymmetric (i.e. *sLag*) fractional three-cycles bounded in their length by the RR tadpole cancellation conditions and by the allowed values for the complex structure moduli, which encode the relative angles between the different root lattices as well as between the generators within each A_3 lattice, reveals — in analogy to the factorisable cases [42, 46, 48] — the existence of several dualities, which lead to identical physics for different choices of lattice orientations under $\mathcal{R}$. More precisely, on $A_3 \times A_3$ we found a duality relation between the $\mathbf{AAA}$ and $\mathbf{BAB}$ lattices, leaving three independent choices. For the $A_3 \times A_1 \times B_2$ lattice, there are four pairwise duality relations ($\mathbf{A_a AA}$ and $\mathbf{A_a AB}$, $\mathbf{A_a BA}$ and $\mathbf{A_a BB}$, $\mathbf{A_b AA}$ and $\mathbf{A_b BB}$, $\mathbf{A_b BA}$ and $\mathbf{A_b AB}$), leaving only four independent choices.

After computing the *sLag* three-cycles, in order to ascertain our results, we cross-checked agreement of the RR tadpole cancellation conditions among our new purely geometric derivation as well as via the 'old' CFT method, in particular for the special D6-brane configurations on top of the O6-planes in [63], compared to which we generalised the CFT results to arbitrary values of the angles inside the A_3 lattices and the angle between the A_3 and the A_1 lattices. For the $A_3 \times A_3$ lattices and the $\mathbf{a}$-lattices of $A_3 \times A_1 \times B_2$, our results derived in a twofold, mutually agreeing way (mostly) coincide with the results listed in [63], while those corresponding to the $\mathbf{b}$-type lattices of $A_3 \times A_1 \times B_2$ are newly found here.

With the full list of allowed *sLag* three-cycles at hand, we proceeded to search for local and global semi-realistic Pati-Salam models on both types of lattices. The $A_3 \times A_3$ lattices happened to be very restricted — e.g. by the small number of available three-cycles — and therefore unsuitable for model building. But the $A_3 \times A_1 \times B_2$ lattice with different orientations provided a very rich class of backgrounds with ample potential for model building. Although the search for global Pati-Salam models — to which we restricted ourselves here since the K-theory constraints are trivially fulfilled in that case — with three generations did not bear any fruit, many models with two and four generations were found. From a qualitative point of view, our results are in agreement with [99] — which studied these non-factorisable orbifolds in the context of the heterotic string — in the sense that the $A_3 \times A_1 \times B_2$ lattice is the most promising non-factorisable one for model building.

Our first model searches typically lead to globally consistent models, where one or more stacks of D-branes wrap three-cycles invariant under the anti-holomorphic involution $\mathcal{R}$. While it is well known that in such cases an enhancement of the gauge group

U(N) $\hookrightarrow$ USp($2N$) or SO($2N$) occurs, the correct distinction can — with the generally available model building techniques to date — only be done by computing open string CFT amplitudes such as the gauge thresholds for factorisable backgrounds in [45, 46, 48, 83] and reading off the correct sign for the orientifold projection from the Möbius strip contribution to either the one-loop beta function coefficient or to the RR tadpoles. Our finding in section 4, that fractional three-cycles can be rewritten in a factorised form, suggests that the CFT methods can be straightforwardly generalised to the non-factorisable backgrounds of $T^6/\mathbb{Z}_4$ discussed here from a purely geometric viewpoint. By fully developing the corresponding CFT, not only the compete chiral plus vector-like matter spectrum can be determined, but also the low-energy effective action can (in principle) be derived. Identifying all probe D-branes supporting USp(2) gauge groups by means of CFT techniques is furthermore necessary to determine the K-theory constraints for all future Standard Model or GUT model building.

Last but not least, it will be interesting to extend the methods for studying non-factorisable orbifolds to other point groups $\mathbb{Z}_{N \neq 4}$, and to incorporate closed string fluxes and study if particle physics models with (nearly) complete stabilisation of the closed string moduli are within reach.

Acknowledgments

A More Pati-Salam models

In this appendix, we provide additional explicit examples of global Pati-Salam models with two and four generations on the $A_3 \times A_1 \times B_2$ lattice.

A.1 2 generations

In the main text, we presented a global model where one of the left- or right-symmetric groups of the Pati-Salam gauge group is provided by an enhanced SO(2)$_{L/R}$ or USp(2)$_{L/R}$ symmetry. We also found global models where none or both left- and/or right-symmetric groups are replaced by an enhanced gauge symmetry; we will show an example of each of type in the following.

Tables 20 and 21 show the D6-branes and chiral spectrum, respectively, of a global Pati-Salam model with visible gauge group U(4) $\times$ U(2) $\times$ U(2).

Tables 22 and 23 show the D6-branes and chiral spectrum, respectively, of a global Pati-Salam model with visible gauge group U(4) $\times$ USp/SO(2) $\times$ USp/SO(2).

D6-branes configuration for a two generation PS-model on $A_3 \times A_1 \times B_2$-orientifold		
Stack	$(m^1, n^1, p^1, q^1) \times (m^2, n^2, p^2, q^2) \times (m^3, n^3)$	Homology cycle
$\mathrm{U}(4)_a$	$(1, 2, 1, 0) \times (0, 0, 0, 1) \times (0, 1)$	$\bar{\gamma}_2 + \bar{\gamma}_3$
$\mathrm{U}(2)_b$	$(1, 1, 0, 0) \times (1, 0, 1, -1) \times (0, -1)$	$\frac{1}{2}(\gamma_1 + \gamma_2 - \gamma_3 - \gamma_4 + \bar{\gamma}_1 + \bar{\gamma}_2 + \bar{\gamma}_3 + \bar{\gamma}_4)$
$\mathrm{U}(2)_c$	$(1, 1, 0, 0) \times (1, 0, 1, -1) \times (0, -1)$	$\frac{1}{2}(\gamma_1 + \gamma_2 + \gamma_3 + \gamma_4 + \bar{\gamma}_1 + \bar{\gamma}_2 - \bar{\gamma}_3 - \bar{\gamma}_4)$
$\mathrm{U}(2)_{h_1}$	$(0, 1, 1, 0) \times (0, 0, 0, 1) \times (1, 2)$	$\bar{\gamma}_2 - \bar{\gamma}_3 + \bar{\gamma}_4$
$\mathrm{USp/SO}(4)_{h_2}$	$(1, 1, 0, 0) \times (1, 0, 1, 0) \times (-1, -2)$	γ_1

Table 20. D6-branes for a global two generation PS-model on the $\mathbf{A_aBB}$-lattice with $u_2 = 1$.

Chiral spectrum of a two generation PS-model on $A_3 \times A_1 \times B_2$-orientifold	
Sector	$\mathrm{SU}(4)_a \times \mathrm{SU}(2)_b \times \mathrm{SU}(2)_c \times \mathrm{SU}(2)_{h_1} \times \mathrm{USp/SO}(4)_{h_2} \times \mathrm{U}(1)^4$
ab	$2 \times (4, \bar{2}, 1, 1, 1)_{(1, -1, 0, 0)}$
ac'	$2 \times (\bar{4}, 1, \bar{2}, 1, 1)_{(-1, 0, -1, 0)}$
bc'	$2 \times (1, \bar{2}, \bar{2}, 1, 1)_{(0, -1, -1, 0)}$
bb'	$2 \times (1, 3, 1, 1, 1)_{(0, 0, 0, 0)}$
cc'	$2 \times (1, 1, 3, 1, 1)_{(0, 0, 0, 0)}$
bh_1'	$2 \times (1, \bar{2}, 1, \bar{2}, 1)_{(0, -1, 0, -1)}$
ch_1	$2 \times (1, 1, \bar{2}, 2, 1)_{(0, 0, -1, 1)}$
$bh_2 = bh_2'$	$(1, 2, 1, 1, \bar{4})_{(0, 1, 0, 0)}$
$ch_2 = ch_2'$	$(1, 1, 2, 1, \bar{4})_{(0, 0, 1, 0)}$

Table 21. Chiral spectrum of the two generation $\mathrm{U}(4) \times \mathrm{U}(2) \times \mathrm{U}(2) \times \mathrm{U}(2) \times \mathrm{USp/SO}(4)$-PS model with D-brane configuration displayed in table 20.

D6-branes configuration for a two generation PS-model on $A_3 \times A_1 \times B_2$-orientifold		
Stack	$(m^1, n^1, p^1, q^1) \times (m^2, n^2, p^2, q^2) \times (m^3, n^3)$	Homology cycle
$\mathrm{U}(4)_a$	$(1, 2, 1, 0) \times (0, 0, 0, 1) \times (0, 1)$	$\bar{\gamma}_2 - \bar{\gamma}_4$
$\mathrm{USp/SO}(2)_b$	$(1, 1, 0, 0) \times (1, 0, 1, 0) \times (-1, -2)$	$\gamma_1 + \gamma_3 + \gamma_4$
$\mathrm{USp/SO}(2)_c$	$(1, 1, 0, 0) \times (1, 0, 1, 0) \times (-1, -2)$	$\gamma_1 - \gamma_3 - \gamma_4$
$\mathrm{U}(4)_{h_1}$	$(1, 2, 1, 0) \times (0, 0, 0, 1) \times (0, 1)$	$\bar{\gamma}_2 + \bar{\gamma}_4$
$\mathrm{USp/SO}(2)_{h_2}$	$(1, 1, 0, 0) \times (1, 0, 1, 0) \times (-1, -2)$	γ_1

Table 22. D6-branes for a global two generation PS-model on the $\mathbf{A_aBB}$-lattice with non-fixed u_2.

A.2 4 generations

As in the previous case, we also found four-generation global Pati-Salam models where none, one or both left- and/or right-symmetric groups are replaced by an enhanced symmetry $\mathrm{SO}(2)_{L/R}$ or $\mathrm{USp}(2)_{L/R}$. Here we will show a concrete example for each of these three cases.

Chiral spectrum of a two generation PS-model on $A_3 \times A_1 \times B_2$-orientifold	
Sector	$\mathrm{SU(4)}_a \times \mathrm{USp/SO(2)}_b \times \mathrm{USp/SO(2)}_c \times \mathrm{SU(4)}_{h_1} \times \mathrm{USp/SO(2)}_{h_2} \times \mathrm{U(1)}^2$
$ab = ab'$	$2 \times (4, \bar{2}, 1, 1, 1)_{(1,0)}$
$ac = ac'$	$2 \times (\bar{4}, 1, 2, 1, 1)_{(-1,0)}$

Table 23. Chiral spectrum of the two generation $\mathrm{U(4)} \times \mathrm{USp/SO(2)} \times \mathrm{USp/SO(2)} \times \mathrm{USp/SO(2)} \times \mathrm{U(4)}$-PS model with D6-brane configuration displayed in table 22.

D6-branes configuration for a four generation PS-model on $A_3 \times A_1 \times B_2$-orientifold		
Stack	$(m^1, n^1, p^1, q^1) \times (m^2, n^2, p^2, q^2) \times (m^3, n^3)$	Homology cycle
U(4)	$(0, 1, 1, 0) \times (0, 0, 0, 1) \times (1, 2)$	$\bar{\gamma}_2 - \bar{\gamma}_3 - \bar{\gamma}_4$
U(2)	$(0, 1, 1, 0) \times (1, 0, 1, -1) \times (0, 1)$	$\frac{1}{2}(\gamma_1 - \gamma_2 + \gamma_3 + \gamma_4 - \bar{\gamma}_1 + \bar{\gamma}_2 + \bar{\gamma}_3 + \bar{\gamma}_4)$
U(2)	$(1, 1, 0, 0) \times (1, 0, 1, -1) \times (0, -1)$	$\frac{1}{2}(\gamma_1 + \gamma_2 - \gamma_3 - \gamma_4 + \bar{\gamma}_1 + \bar{\gamma}_2 + \bar{\gamma}_3 + \bar{\gamma}_4)$
$\mathrm{U(2)}_{h_1}$	$(0, 1, 1, 0) \times (0, 0, 0, 1) \times (1, 2)$	$\bar{\gamma}_2 - \bar{\gamma}_3 + \bar{\gamma}_4$
$\mathrm{USp/SO(4)}_{h_2}$	$(1, 1, 0, 0) \times (1, 0, 1, 0) \times (-1, -2)$	γ_1

Table 24. D6-branes for a global four generation PS-model on the $\mathbf{A_aBB}$-lattice with $u_2 = 1$.

Chiral spectrum of a four generation PS-model on $A_3 \times A_1 \times B_2$-orientifold	
Sector	$\mathrm{SU(4)}_a \times \mathrm{SU(2)}_b \times \mathrm{SU(2)}_c \times \mathrm{SU(2)}_{h_1} \times \mathrm{USp/SO(4)}_{h_2} \times \mathrm{U(1)}^4$
ab	$(4, \bar{2}, 1, 1, 1)_{(1,-1,0,0)}$
ab'	$3 \times (4, 2, 1, 1, 1)_{(1,1,0,0)}$
ac	$(\bar{4}, 1, 2, 1, 1)_{(-1,0,1,0)}$
ac'	$3 \times (\bar{4}, 1, \bar{2}, 1, 1)_{(-1,0,-1,0)}$
bc	$2 \times (1, 2, \bar{2}, 1, 1)_{(0,1,-1,0)}$
bb'	$2 \times (1, 3, 1, 1, 1)_{(0,0,0,0)}$
cc'	$2 \times (1, 1, 3, 1, 1)_{(0,0,0,0)}$
bh'_1	$2 \times (1, \bar{2}, 1, \bar{2}, 1)_{(0,-1,0,-1)}$
ch_1	$2 \times (1, 1, \bar{2}, 2, 1)_{(0,0,-1,1)}$
$bh_2 = bh'_2$	$(1, 2, 1, 1, \bar{4})_{(0,1,0,0)}$
$ch_2 = ch'_2$	$(1, 1, 2, 1, \bar{4})_{(0,0,1,0)}$

Table 25. Chiral spectrum of the four generation $\mathrm{U(4)} \times \mathrm{U(2)} \times \mathrm{U(2)} \times \mathrm{USp/SO(4)} \times \mathrm{U(2)}$-PS model with D6-brane configuration displayed in table 24.

Tables 24 and 25 show the D6-brane configuration and chiral spectrum, respectively, of a Pati-Salam model with visible sector $\mathrm{U(4)} \times \mathrm{U(2)} \times \mathrm{U(2)}$.

Tables 26 and 27 show the D6-brane configuration and chiral spectrum, respectively, of a Pati-Salam model with visible sector $\mathrm{U(4)} \times \mathrm{U(2)} \times \mathrm{USp/SO(2)}$.

Tables 28 and 29 show the D6-brane configuration and chiral spectrum, respectively, of a Pati-Salam model with visible sector $\mathrm{U(4)} \times \mathrm{USp/SO(2)} \times \mathrm{USp/SO(2)}$.

D6-branes configuration a for four generation PS-model on $A_3 \times A_1 \times B_2$-orientifold		
Stack	$(m^1, n^1, p^1, q^1) \times (m^2, n^2, p^2, q^2) \times (m^3, n^3)$	Homology cycle
U(4)$_a$	$(0,1,1,0) \times (0,0,0,1) \times (1,2)$	$\bar{\gamma}_2 + \bar{\gamma}_3 + \bar{\gamma}_4$
U(2)$_b$	$(0,1,1,0) \times (1,0,1,1) \times (0,1)$	$\frac{1}{2}(\gamma_1 - \gamma_2 - \gamma_3 - \gamma_4 - \bar{\gamma}_1 + \bar{\gamma}_2 - \bar{\gamma}_3 - \bar{\gamma}_4)$
USp/SO(2)$_c$	$(1,1,0,0) \times (1,0,1,0) \times (-1,-2)$	$\gamma_1 + \gamma_3 + \gamma_4$
U(3)$_{h_1}$	$(0,1,1,0) \times (0,0,0,1) \times (1,2)$	$\bar{\gamma}_2 + \bar{\gamma}_3 - \bar{\gamma}_4$
USp/SO(2)$_{h_2}$	$(1,1,0,0) \times (1,0,1,0) \times (-1,-2)$	γ_1

Table 26. D6-branes for a global four generation PS-model on the **A_aBB**-lattice with $u_2 = 1$.

Chiral spectrum of a four generation PS-model on $A_3 \times A_1 \times B_2$-orientifold	
Sector	$\mathrm{SU(4)}_a \times \mathrm{SU(2)}_b \times \mathrm{USp/SO(2)}_c \times \mathrm{SU(3)}_{h_1} \times \mathrm{USp/SO(2)}_{h_2} \times \mathrm{U(1)}^3$
ab	$(4, \bar{2}, 1, 1, 1)_{(1,-1,0)}$
ab'	$3 \times (4, 2, 1, 1, 1)_{(1,1,0)}$
$ac = ac'$	$4 \times (\bar{4}, 1, 2, 1, 1)_{(-1,0,0)}$
$bc = bc'$	$(1, 2, \bar{2}, 1, 1)_{(0,1,0)}$
bb'	$2 \times (1, 3, 1, 1, 1)_{(0,0,0)}$
bh_1	$(1, 2, 1, \bar{3}, 1)_{(0,1,-1)}$
bh_1'	$(1, 2, 1, 3, 1)_{(0,1,1)}$

Table 27. Chiral spectrum of the four generation $\mathrm{U(4)} \times \mathrm{U(2)} \times \mathrm{USp/SO(2)} \times \mathrm{U(3)} \times \mathrm{USp/SO(2)}$-PS model with D6-brane configuration given in table 26.

D6-branes configuration for a four generation PS-model on $A_3 \times A_1 \times B_2$-orientifold		
Stack	$(m^1, n^1, p^1, q^1) \times (m^2, n^2, p^2, q^2) \times (m^3, n^3)$	Homology cycle
U(4)$_a$	$(1,0,-1,0) \times (0,0,0,1) \times (-1,-2)$	$-\bar{\gamma}_1 + \bar{\gamma}_2 + 2\bar{\gamma}_4$
USp/SO(2)$_b$	$(0,1,0,0) \times (1,0,1,0) \times (1,2)$	$\frac{1}{2}\gamma_1 + \frac{1}{2}\gamma_2 - \gamma_4$
USp/SO(2)$_c$	$(0,1,0,0) \times (1,0,1,0) \times (1,2)$	$\frac{1}{2}\gamma_1 + \frac{1}{2}\gamma_2 + \gamma_4$
USp/SO(4)$_h$	$(0,1,0,0) \times (1,0,1,0) \times (1,2)$	$\frac{1}{2}\gamma_1 + \frac{1}{2}\gamma_2$

Table 28. D6-branes for a global four generation PS-model one the **A_aAB**-lattice with non-fixed u_2.

Chiral spectrum of a four generation PS-model on $A_3 \times A_1 \times B_2$-orientifold	
Sector	$\mathrm{SU(4)}_a \times \mathrm{USp/SO(2)}_b \times \mathrm{USp/SO(2)}_c \times \mathrm{USp/SO(4)}_h \times \mathrm{U(1)}$
$ab = ab'$	$4 \times (4, \bar{2}, 1, 1)_{+1}$
$ac = ac'$	$4 \times (\bar{4}, 1, 2, 1)_{-1}$

Table 29. Chiral spectrum of the four generation $\mathrm{U(4)} \times \mathrm{USp/SO(2)} \times \mathrm{USp/SO(2)} \times \mathrm{USp/SO(4)}$-PS model with D6-brane configuration displayed in table 28.

References

[1] P. Candelas, G.T. Horowitz, A. Strominger and E. Witten, *Vacuum configurations for superstrings*, *Nucl. Phys.* **B 258** (1985) 46 [INSPIRE].

[2] E. Witten, *Symmetry breaking patterns in superstring models*, *Nucl. Phys.* **B 258** (1985) 75 [INSPIRE].

[3] L.E. Ibáñez, J.E. Kim, H.P. Nilles and F. Quevedo, *Orbifold compactifications with three families of* $SU(3) \times SU(2) \times U(1)^n$, *Phys. Lett.* **B 191** (1987) 282 [INSPIRE].

[4] O. Lebedev et al., *A mini-landscape of exact MSSM spectra in heterotic orbifolds*, *Phys. Lett.* **B 645** (2007) 88 [hep-th/0611095] [INSPIRE].

[5] O. Lebedev, H.P. Nilles, S. Ramos-Sanchez, M. Ratz and P.K.S. Vaudrevange, *Heterotic mini-landscape (II): completing the search for MSSM vacua in a* Z_6 *orbifold*, *Phys. Lett.* **B 668** (2008) 331 [arXiv:0807.4384] [INSPIRE].

[6] H.P. Nilles, S. Ramos-Sanchez, P.K.S. Vaudrevange and A. Wingerter, *The orbifolder: a tool to study the low energy effective theory of heterotic orbifolds*, *Comput. Phys. Commun.* **183** (2012) 1363 [arXiv:1110.5229] [INSPIRE].

[7] K.-S. Choi, S. Groot Nibbelink and M. Trapletti, *Heterotic* SO(32) *model building in four dimensions*, *JHEP* **12** (2004) 063 [hep-th/0410232] [INSPIRE].

[8] A. Bak, V. Bouchard and R. Donagi, *Exploring a new peak in the heterotic landscape*, *JHEP* **06** (2010) 108 [arXiv:0811.1242] [INSPIRE].

[9] L.B. Anderson, J. Gray, A. Lukas and E. Palti, *Two hundred heterotic standard models on smooth Calabi-Yau threefolds*, *Phys. Rev.* **D 84** (2011) 106005 [arXiv:1106.4804] [INSPIRE].

[10] L.B. Anderson, J. Gray, A. Lukas and E. Palti, *Heterotic line bundle standard models*, *JHEP* **06** (2012) 113 [arXiv:1202.1757] [INSPIRE].

[11] L.B. Anderson, A. Constantin, J. Gray, A. Lukas and E. Palti, *A comprehensive scan for heterotic* SU(5) *GUT models*, *JHEP* **01** (2014) 047 [arXiv:1307.4787] [INSPIRE].

[12] S. Groot Nibbelink, O. Loukas, F. Ruehle and P.K.S. Vaudrevange, *Infinite number of MSSMs from heterotic line bundles?*, *Phys. Rev.* **D 92** (2015) 046002 [arXiv:1506.00879] [INSPIRE].

[13] J. Polchinski, *Dirichlet branes and Ramond-Ramond charges*, *Phys. Rev. Lett.* **75** (1995) 4724 [hep-th/9510017] [INSPIRE].

[14] C. Vafa and E. Witten, *A strong coupling test of S duality*, *Nucl. Phys.* **B 431** (1994) 3 [hep-th/9408074] [INSPIRE].

[15] J. Polchinski and E. Witten, *Evidence for heterotic-type I string duality*, *Nucl. Phys.* **B 460** (1996) 525 [hep-th/9510169] [INSPIRE].

[16] J.H. Schwarz, *The power of M-theory*, *Phys. Lett.* **B 367** (1996) 97 [hep-th/9510086] [INSPIRE].

[17] C. Vafa, *Evidence for F-theory*, *Nucl. Phys.* **B 469** (1996) 403 [hep-th/9602022] [INSPIRE].

[18] L.E. Ibáñez and A.M. Uranga, *String theory and particle physics: an introduction to string phenomenology*, Cambridge University Press, Cambridge U.K. (2012) [INSPIRE].

[19] D. Joyce, *Lectures on Calabi-Yau and special Lagrangian geometry*, `math.DG/0108088` [INSPIRE].

[20] D. Joyce, *Lectures on special Lagrangian geometry*, `math.DG/0111111`.

[21] E. Palti, *Model building with intersecting D6-branes on smooth Calabi-Yau manifolds*, *JHEP* **04** (2009) 099 [`arXiv:0902.3546`] [INSPIRE].

[22] L.E. Ibáñez, F. Marchesano and R. Rabadán, *Getting just the standard model at intersecting branes*, *JHEP* **11** (2001) 002 [`hep-th/0105155`] [INSPIRE].

[23] D. Cremades, L.E. Ibáñez and F. Marchesano, *SUSY quivers, intersecting branes and the modest hierarchy problem*, *JHEP* **07** (2002) 009 [`hep-th/0201205`] [INSPIRE].

[24] D. Cremades, L.E. Ibáñez and F. Marchesano, *Intersecting brane models of particle physics and the Higgs mechanism*, *JHEP* **07** (2002) 022 [`hep-th/0203160`] [INSPIRE].

[25] M. Cvetič, G. Shiu and A.M. Uranga, *Three family supersymmetric standard-like models from intersecting brane worlds*, *Phys. Rev. Lett.* **87** (2001) 201801 [`hep-th/0107143`] [INSPIRE].

[26] M. Cvetič, G. Shiu and A.M. Uranga, *Chiral four-dimensional $N = 1$ supersymmetric type 2A orientifolds from intersecting D6 branes*, *Nucl. Phys.* **B 615** (2001) 3 [`hep-th/0107166`] [INSPIRE].

[27] R. Blumenhagen, M. Cvetič, P. Langacker and G. Shiu, *Toward realistic intersecting D-brane models*, *Ann. Rev. Nucl. Part. Sci.* **55** (2005) 71 [`hep-th/0502005`] [INSPIRE].

[28] F. Gmeiner, R. Blumenhagen, G. Honecker, D. Lüst and T. Weigand, *One in a billion: MSSM-like D-brane statistics*, *JHEP* **01** (2006) 004 [`hep-th/0510170`] [INSPIRE].

[29] R. Blumenhagen, B. Körs, D. Lüst and S. Stieberger, *Four-dimensional string compactifications with D-branes, orientifolds and fluxes*, *Phys. Rept.* **445** (2007) 1 [`hep-th/0610327`] [INSPIRE].

[30] F. Gmeiner and M. Stein, *Statistics of* SU(5) *D-brane models on a type-II orientifold*, *Phys. Rev.* **D 73** (2006) 126008 [`hep-th/0603019`] [INSPIRE].

[31] G. Honecker, *Chiral supersymmetric models on an orientifold of $Z_4 \times Z_2$ with intersecting D6-branes*, *Nucl. Phys.* **B 666** (2003) 175 [`hep-th/0303015`] [INSPIRE].

[32] G. Honecker, *Supersymmetric intersecting D6-branes and chiral models on the $T^6/(\mathbb{Z}_4 \times \mathbb{Z}_2)$ orbifold*, in Proceedings of *String phenomenology. 2nd International Conference*, Durham U.K., 29 Jul–4 Aug 2003, pp. 191–198.

[33] G. Honecker, *Chiral $N = 1$ 4D orientifolds with D-branes at angles*, *Mod. Phys. Lett.* **A 19** (2004) 1863 [`hep-th/0407181`] [INSPIRE].

[34] R. Blumenhagen, L. Görlich and T. Ott, *Supersymmetric intersecting branes on the type IIA T^6/Z_4 orientifold*, *JHEP* **01** (2003) 021 [`hep-th/0211059`] [INSPIRE].

[35] G. Honecker and T. Ott, *Getting just the supersymmetric standard model at intersecting branes on the $\mathbb{Z}_6$ orientifold*, *Phys. Rev.* **D 70** (2004) 126010 [*Erratum ibid.* **D 71** (2005) 069902] [`hep-th/0404055`] [INSPIRE].

[36] F. Gmeiner, D. Lüst and M. Stein, *Statistics of intersecting D-brane models on $T^6/\mathbb{Z}_6$*, *JHEP* **05** (2007) 018 [`hep-th/0703011`] [INSPIRE].

[37] F. Gmeiner and G. Honecker, *Complete gauge threshold corrections for intersecting fractional D6-branes: the $\mathbb{Z}_6$ and $\mathbb{Z}_6'$ standard models*, *Nucl. Phys.* **B 829** (2010) 225 [arXiv:0910.0843] [INSPIRE].

[38] D. Bailin and A. Love, *Towards the supersymmetric standard model from intersecting D6-branes on the $\mathbb{Z}_6'$ orientifold*, *Nucl. Phys.* **B 755** (2006) 79 [*Erratum ibid.* **B 783** (2007) 176] [hep-th/0603172] [INSPIRE].

[39] D. Bailin and A. Love, *Almost the supersymmetric standard model from intersecting D6-branes on the $\mathbb{Z}_6'$ orientifold*, *Phys. Lett.* **B 651** (2007) 324 [*Erratum ibid.* **B 658** (2008) 292] [arXiv:0705.0646] [INSPIRE].

[40] F. Gmeiner and G. Honecker, *Mapping an island in the landscape*, *JHEP* **09** (2007) 128 [arXiv:0708.2285] [INSPIRE].

[41] D. Bailin and A. Love, *Constructing the supersymmetric standard model from intersecting D6-branes on the $\mathbb{Z}_6'$ orientifold*, *Nucl. Phys.* **B 809** (2009) 64 [arXiv:0801.3385] [INSPIRE].

[42] F. Gmeiner and G. Honecker, *Millions of standard models on $\mathbb{Z}_6'$?*, *JHEP* **07** (2008) 052 [arXiv:0806.3039] [INSPIRE].

[43] D. Bailin and A. Love, *Intersecting D6-branes on the $\mathbb{Z}_{12}$-II orientifold*, *JHEP* **01** (2014) 009 [arXiv:1310.8215] [INSPIRE].

[44] R. Blumenhagen, M. Cvetič, F. Marchesano and G. Shiu, *Chiral D-brane models with frozen open string moduli*, *JHEP* **03** (2005) 050 [hep-th/0502095] [INSPIRE].

[45] S. Förste and G. Honecker, *Rigid D6-branes on $T^6/(\mathbb{Z}_2 \times \mathbb{Z}_{2M} \times \Omega\mathcal{R})$ with discrete torsion*, *JHEP* **01** (2011) 091 [arXiv:1010.6070] [INSPIRE].

[46] G. Honecker, M. Ripka and W. Staessens, *The importance of being rigid: D6-brane model building on $T^6/\mathbb{Z}_2 \times \mathbb{Z}_6'$ with discrete torsion*, *Nucl. Phys.* **B 868** (2013) 156 [arXiv:1209.3010] [INSPIRE].

[47] G. Honecker and W. Staessens, *D6-brane model building and discrete symmetries on $T^6/(\mathbb{Z}_2 \times \mathbb{Z}_6 \times \Omega\mathcal{R})$ with discrete torsion*, PoS(Corfu2012)107 [arXiv:1303.6845] [INSPIRE].

[48] J. Ecker, G. Honecker and W. Staessens, *Rigour and rigidity: systematics on particle physics D6-brane models on $\mathbb{Z}_2 \times \mathbb{Z}_6$*, *Fortschr. Phys.* **62** (2014) 981 [arXiv:1409.1236] [INSPIRE].

[49] J. Ecker, G. Honecker and W. Staessens, *D6-brane model building on $\mathbb{Z}_2 \times \mathbb{Z}_6$: MSSM-like and left-right symmetric models*, *Nucl. Phys.* **B 901** (2015) 139 [arXiv:1509.00048] [INSPIRE].

[50] G. Honecker, *From stringy particle physics to moduli stabilisation and cosmology*, *Fortschr. Phys.* **64** (2016) 380 [arXiv:1510.08443] [INSPIRE].

[51] M. Blaszczyk, G. Honecker and I. Koltermann, *Circling the square: deforming fractional D-branes in type-II/$\Omega\mathcal{R}$ orientifolds*, *JHEP* **07** (2014) 124 [arXiv:1403.2394] [INSPIRE].

[52] M. Blaszczyk, G. Honecker and I. Koltermann, *Deformations on tilted tori and moduli stabilisation at the orbifold point*, *JHEP* **11** (2015) 019 [arXiv:1507.07568] [INSPIRE].

[53] I. Koltermann, M. Blaszczyk and G. Honecker, *Deforming D-brane models on $T^6/(\mathbb{Z}_2 \times \mathbb{Z}_{2M})$ orbifolds*, *Fortschr. Phys.* **64** (2016) 412 [arXiv:1511.03549] [INSPIRE].

[54] M. Graña, *Flux compactifications in string theory: a comprehensive review*, *Phys. Rept.* **423** (2006) 91 [hep-th/0509003] [INSPIRE].

[55] P. Koerber, *Lectures on generalized complex geometry for physicists*, *Fortschr. Phys.* **59** (2011) 169 [arXiv:1006.1536] [InSPIRE].

[56] M. Larfors, *Generalised geometry and flux vacua*, *Fortschr. Phys.* **64** (2016) 354 [arXiv:1511.04595] [InSPIRE].

[57] M. Ihl and T. Wrase, *Towards a realistic type IIA $T^6/\mathbb{Z}_4$ orientifold model with background fluxes. Part 1. Moduli stabilization*, *JHEP* **07** (2006) 027 [hep-th/0604087] [InSPIRE].

[58] M. Ihl, D. Robbins and T. Wrase, *Toroidal orientifolds in IIA with general NS-NS fluxes*, *JHEP* **08** (2007) 043 [arXiv:0705.3410] [InSPIRE].

[59] D. Bailin and A. Love, *Stabilising the supersymmetric standard model on the $\mathbb{Z}_6'$ orientifold*, *Nucl. Phys.* **B 854** (2012) 700 [arXiv:1104.3522] [InSPIRE].

[60] P.G. Camara, A. Font and L.E. Ibáñez, *Fluxes, moduli fixing and MSSM-like vacua in a simple IIA orientifold*, *JHEP* **09** (2005) 013 [hep-th/0506066] [InSPIRE].

[61] G. Aldazabal, P.G. Camara, A. Font and L.E. Ibáñez, *More dual fluxes and moduli fixing*, *JHEP* **05** (2006) 070 [hep-th/0602089] [InSPIRE].

[62] F. Marchesano, *D6-branes and torsion*, *JHEP* **05** (2006) 019 [hep-th/0603210] [InSPIRE].

[63] R. Blumenhagen, J.P. Conlon and K. Suruliz, *Type IIA orientifolds on general supersymmetric $\mathbb{Z}_N$ orbifolds*, *JHEP* **07** (2004) 022 [hep-th/0404254] [InSPIRE].

[64] T. Kimura, M. Ohta and K.-J. Takahashi, *Type IIA orientifolds and orbifolds on non-factorizable tori*, *Nucl. Phys.* **B 798** (2008) 89 [arXiv:0712.2281] [InSPIRE].

[65] S. Förste, C. Timirgaziu and I. Zavala, *Orientifold's landscape: non-factorisable six-tori*, *JHEP* **10** (2007) 025 [arXiv:0707.0747] [InSPIRE].

[66] S. Förste and I. Zavala, *Oddness from rigidness*, *JHEP* **07** (2008) 086 [arXiv:0806.2328] [InSPIRE].

[67] S. Förste and C. Liyanage, *Yukawa couplings for intersecting D-branes on non-factorisable tori*, *JHEP* **03** (2015) 110 [arXiv:1412.3645] [InSPIRE].

[68] A. Seifert and G. Honecker, *Model building on the non-factorisable type IIA $T^6/(\mathbb{Z}_4 \times \Omega\mathcal{R})$ orientifold*, *Fortschr. Phys.* **64** (2016) 416 [arXiv:1511.03075] [InSPIRE].

[69] T.P.T. Dijkstra, L.R. Huiszoon and A.N. Schellekens, *Chiral supersymmetric standard model spectra from orientifolds of Gepner models*, *Phys. Lett.* **B 609** (2005) 408 [hep-th/0403196] [InSPIRE].

[70] T.P.T. Dijkstra, L.R. Huiszoon and A.N. Schellekens, *Supersymmetric standard model spectra from RCFT orientifolds*, *Nucl. Phys.* **B 710** (2005) 3 [hep-th/0411129] [InSPIRE].

[71] P. Anastasopoulos, T.P.T. Dijkstra, E. Kiritsis and A.N. Schellekens, *Orientifolds, hypercharge embeddings and the standard model*, *Nucl. Phys.* **B 759** (2006) 83 [hep-th/0605226] [InSPIRE].

[72] P. Anastasopoulos, G.K. Leontaris, R. Richter and A.N. Schellekens, *SU(5) D-brane realizations, Yukawa couplings and proton stability*, *JHEP* **12** (2010) 011 [arXiv:1010.5188] [InSPIRE].

[73] D. Lüst and S. Stieberger, *Gauge threshold corrections in intersecting brane world models*, *Fortschr. Phys.* **55** (2007) 427 [hep-th/0302221] [InSPIRE].

[74] S.A. Abel and A.W. Owen, *Interactions in intersecting brane models*,
Nucl. Phys. **B 663** (2003) 197 [`hep-th/0303124`] [ɪɴSPIRE].

[75] M. Cvetič and I. Papadimitriou, *Conformal field theory couplings for intersecting D-branes on orientifolds*, *Phys. Rev.* **D 68** (2003) 046001 [*Erratum ibid.* **D 70** (2004) 029903] [`hep-th/0303083`] [ɪɴSPIRE].

[76] S.A. Abel and A.W. Owen, *N point amplitudes in intersecting brane models*,
Nucl. Phys. **B 682** (2004) 183 [`hep-th/0310257`] [ɪɴSPIRE].

[77] D. Lüst, P. Mayr, R. Richter and S. Stieberger, *Scattering of gauge, matter and moduli fields from intersecting branes*, *Nucl. Phys.* **B 696** (2004) 205 [`hep-th/0404134`] [ɪɴSPIRE].

[78] N. Akerblom, R. Blumenhagen, D. Lüst and M. Schmidt-Sommerfeld, *Instantons and holomorphic couplings in intersecting D-brane models*, *JHEP* **08** (2007) 044 [`arXiv:0705.2366`] [ɪɴSPIRE].

[79] R. Blumenhagen and M. Schmidt-Sommerfeld, *Gauge thresholds and Kähler metrics for rigid intersecting D-brane models*, *JHEP* **12** (2007) 072 [`arXiv:0711.0866`] [ɪɴSPIRE].

[80] G. Honecker, *Kähler metrics and gauge kinetic functions for intersecting D6-branes on toroidal orbifolds — the complete perturbative story*, *Fortschr. Phys.* **60** (2012) 243 [`arXiv:1109.3192`] [ɪɴSPIRE].

[81] G. Honecker, *Towards exact field theory results for the standard model on fractional D6-branes*, `PoS(EPS-HEP2011)129` [`arXiv:1109.6533`] [ɪɴSPIRE].

[82] M. Berg, M. Haack and J.U. Kang, *One-loop Kähler metric of D-branes at angles*,
JHEP **11** (2012) 091 [`arXiv:1112.5156`] [ɪɴSPIRE].

[83] G. Honecker and W. Staessens, *To tilt or not to tilt: discrete gauge symmetries in global intersecting D-brane models*, *JHEP* **10** (2013) 146 [`arXiv:1303.4415`] [ɪɴSPIRE].

[84] D. Lüst, S. Reffert, E. Scheidegger and S. Stieberger, *Resolved toroidal orbifolds and their orientifolds*, *Adv. Theor. Math. Phys.* **12** (2008) 67 [`hep-th/0609014`] [ɪɴSPIRE].

[85] M. Spalinski, *Duality transformations in twisted Narain compactifications*,
Nucl. Phys. **B 377** (1992) 339 [ɪɴSPIRE].

[86] R. Blumenhagen, V. Braun, B. Körs and D. Lüst, *Orientifolds of K3 and Calabi-Yau manifolds with intersecting D-branes*, *JHEP* **07** (2002) 026 [`hep-th/0206038`] [ɪɴSPIRE].

[87] M. Cvetič and I. Papadimitriou, *More supersymmetric standard-like models from intersecting D6-branes on type IIA orientifolds*, *Phys. Rev.* **D 67** (2003) 126006 [`hep-th/0303197`] [ɪɴSPIRE].

[88] M. Cvetič, T. Li and T. Liu, *Supersymmetric Pati-Salam models from intersecting D6-branes: a road to the standard model*, *Nucl. Phys.* **B 698** (2004) 163 [`hep-th/0403061`] [ɪɴSPIRE].

[89] C.-M. Chen, T. Li and D.V. Nanopoulos, *Type IIA Pati-Salam flux vacua*,
Nucl. Phys. **B 740** (2006) 79 [`hep-th/0601064`] [ɪɴSPIRE].

[90] L.J. Dixon, J.A. Harvey, C. Vafa and E. Witten, *Strings on orbifolds*,
Nucl. Phys. **B 261** (1985) 678 [ɪɴSPIRE].

[91] L.J. Dixon, J.A. Harvey, C. Vafa and E. Witten, *Strings on orbifolds (II)*,
Nucl. Phys. **B 274** (1986) 285 [ɪɴSPIRE].

[92] R. Blumenhagen, L. Görlich and B. Körs, *Supersymmetric orientifolds in 6D with D-branes at angles*, *Nucl. Phys.* **B 569** (2000) 209 [`hep-th/9908130`] [ɪɴSPIRE].

[93] R. Blumenhagen, L. Görlich and B. Körs, *Supersymmetric 4D orientifolds of type IIA with D6-branes at angles*, *JHEP* **01** (2000) 040 [hep-th/9912204] [INSPIRE].

[94] S. Förste, G. Honecker and R. Schreyer, *Supersymmetric $\mathbb{Z}_N \times \mathbb{Z}_M$ orientifolds in 4D with D-branes at angles*, *Nucl. Phys.* **B 593** (2001) 127 [hep-th/0008250] [INSPIRE].

[95] T.W. Grimm and J. Louis, *The effective action of type IIA Calabi-Yau orientifolds*, *Nucl. Phys.* **B 718** (2005) 153 [hep-th/0412277] [INSPIRE].

[96] N. Akerblom, R. Blumenhagen, D. Lüst and M. Schmidt-Sommerfeld, *Thresholds for intersecting D-branes revisited*, *Phys. Lett.* **B 652** (2007) 53 [arXiv:0705.2150] [INSPIRE].

[97] M. Blaszczyk, S. Groot Nibbelink and F. Ruehle, *Gauged linear σ-models for toroidal orbifold resolutions*, *JHEP* **05** (2012) 053 [arXiv:1111.5852] [INSPIRE].

[98] A.M. Uranga, *D-brane probes, RR tadpole cancellation and k-theory charge*, *Nucl. Phys.* **B 598** (2001) 225 [hep-th/0011048] [INSPIRE].

[99] H.P. Nilles and P.K.S. Vaudrevange, *Geography of fields in extra dimensions: string theory lessons for particle physics*, *Mod. Phys. Lett.* **A 30** (2015) 1530008 [arXiv:1403.1597] [INSPIRE].